UNIVERSITY OF OKLAHOMA

GRADUATE COLLEGE

EFFECT OF MULTI-WALLED CARBON NANOTUBES LENGTH, DENSITY, POWDER SIZE AND PRE-TREATMENT METHOD ON ELECTRICAL AND MECHANICAL PROPERTIES OF POLYCARBONATE/MWCNT COMPOSITES

A THESIS

SUBMITTED TO THE GRADUATE FACULTY

in partial fulfillment of the requirements for the

Degree of

MASTER OF SCIENCE

By

JOHN ALEXANDER ZAPATA HINCAPIE
Norman, Oklahoma
2016

EFFECT OF MULTI-WALLED CARBON NANOTUBES LENGTH, DENSITY, POWDER SIZE AND PRE-TREATMENT METHOD ON ELECTRICAL AND MECHANICAL PROPERTIES OF POLYCARBONATE/MWCNT COMPOSITES

A THESIS APPROVED FOR THE
SCHOOL OF CHEMICAL, BIOLOGICAL AND MATERIALS ENGINEERING

BY

_____
Dr. Brian P. Grady, Chair

_____
Dr. Steven Crossley

_____
Dr. Daniel Resasco

This master's thesis is dedicated to:

My mother: Luz Elena Hincapie Preciado

My father: Jhon Jairo Zapata Vargas

My sister: Yuliana Andrea Zapata Hincapie

Acknowledgements

I would like to thank my graduate advisor Dr. Brian P. Grady who has given me the opportunity to come to the United States to pursuit my dreams in higher education. I would also like to thank my graduate committee members: Dr. Daniel Resasco and Dr. Steven Crossley. Thanks also to Alan Miles from the chemical engineering shop. In addition, I want to thank Dr. Benjamin Smith and Dr. Preston Larson for all the time and patience dedicated to strengthen the author's understanding of all microscopy characterization techniques published in this work. Finally, special thanks to all the staff at the Department of Chemical, Biological and Material Science Engineering for providing me invaluable assistance all these years.

Table of Contents

List of Tables

List of Figures

Chapter 1: Introduction

Carbon nanotubes (CNTs) have gained both scientific and commercial attention since Iijima brought their existence in 1991 [1] as a result of their superior mechanical and electrical properties [2] and the relative low concentrations required to enhance these and other properties in polymers. [3-9]. The majority of the studies for CNTs as fillers in a polymer matrix focus on reinforcing mechanical properties, enhancing the thermal conductivity and/or improving the electrical conductivity [10]. In order to fully exploit the exceptional properties of CNTs, it is imperative to find a way to generate a stable and uniform dispersion of the CNTs througout the polymer matrix. However, this dispersion is in practice very difficult to achieve because of physical entanglements and the strong Van der Waals interactions that are present in the CNTs [11] which hinder the formation of a CNT "network-like" structure in the host polymer. Some of the strategies to improve dispersion employ mechanical means (ultrasonication, high shear mixing, external magnetic/electric fields etc.) or are based on manipulating chemically or physically the surface energy of CNTs [12, 13]. Most of these strategies, however, can break or alter the integrity of the CNTs [12-14].

During the manufacture of CNTs, a drying step is required if the nanotubes are to be sold as a powder. Two different drying methods can affect the dispersion of CNTs and hence change the amount of CNT/polymer mixing required. One method is to dry the CNTs in a conventional oven (oven drying) while the second is freeze drying (lyophilization) [15]. Specifically, drying affects the density of the CNT powder. Further, the bigger the length the more CNT entanglements will likely be created and at the same

time more entanglements will result in higher density, meaning that drying differences will have a larger effect on longer tubes. In general, longer tubes and higher density make it more difficult for CNTs to be dispersed throughout a polymer matrix.

In this study fourteen MWCNTs with different lengths, densities, powder size and pre-treatment methods were mixed with polycarbonate, to evaluate their effect on the mechanical and electrical properties of the final composite and these results will be correlated with the state of dispersion at the macro and sub-micron scale. Moreover, since some studies suggest that the intrinsic ability of the CNTs to agglomerate is likely to depend on nanotube diameter [16-18], the diameter of the CNTs was constant to further attempt to show that the aggregation state can also be caused by other variables such as density, length and carbon nanotubes pre-treatment methods.

To the author's knowledge, only one study has been conducted to analyze the effect of oven drying vs freeze drying on PC/MWCNT composites [19]. Furthermore, no studies were found correlating the effect of powder size with the dispersion state of carbon nanotubes.

This thesis is organized in the following structure: The theoretical background is given in Chapter 2 with a general background about CNTs, including a brief discussion on the structure of carbon nanotubes, their main properties and a discussion of the main literature on the effect of length, density and pre-treatment methods on the properties of nanocomposites. Chapter 3 describes the experimental procedures to prepare and characterize the PC/MWCNT composites. Discussion and analysis are given in Chapter 4. Finally, Chapter 5 presents the final remarks and conclusions of this work.

Chapter 2: Literature review

2.1 Structure and properties of carbon nanotubes

2.1.1 Historical Background

The paper written by Radushkevich and Lukyanocich [20] in 1952 is credited to be the first reported discovery of multi-walled carbon nanotubes (MWCNTs) since it showed the first transmission electron microscopy images of carbon nanotubes. However, since nano-filaments in the coal or steel industry were seen as undesirable impurities at that time, MWCNTs did not receive much attention [21] until a paper written by the Japanese Iijima [1] in 1991; which was the first time CNTs were recognized as a new and important material. This seminal publication had several favorable factors that made this scientific work to be noticed by scientists around the world, such as being published in a highly-ranked journal, the fact that this paper followed the discovery of a new allotrope of carbon, C_{60}, in 1985 [22] and a more aware scientific community about how to exploit nanomaterials [23].

Since then, CNTs have been regarded as a material that holds the potential to revolutionize composite materials, energy storage, medicine and more, due to their unique electrical, mechanical, optical, thermal and other properties. Additionally, CNTs have a combination of features like low density, nanoscale dimensions, a very high surface area, high aspect ratio (length/ diameter) and the possibility to vary chemistry along the surface of CNTs [24] that set them apart from other materials.

2.1.2 Structure of carbon nanotubes

The ability of the element carbon to bond with itself and with other atoms in many different combinations form the basis for the vast subject of organic chemistry and life in this planet and yet only until 1985, when Sir Harry Kroto et al. discovered the existence of fullerenes [22], we only knew of two naturally occurring allotropes of carbon: diamond and graphite. Today, carbon nanotubes are considered as one of the naturally occurring allotropes of carbon and are composed of hexagonal carbon rings capped at the end by pentagonal and hexagonal carbon rings or fullerene hemispheres [25]. In perfect form, they have only carbon covalent sp^2 bonds [26].

Carbon nanotubes are categorized as multi-walled carbon nanotubes (MWCNTs) and single-walled carbon nanotubes (SWCNTs). MWCNTs were the first to be brought to the attention of the scientific community in the well-known paper of Iijima [1]. SWCNTs were first observed by Oberlin et al. in 1976 [27] and later reported independently by Bethune et al. [28] and Iijima et al. in 1993 [29].

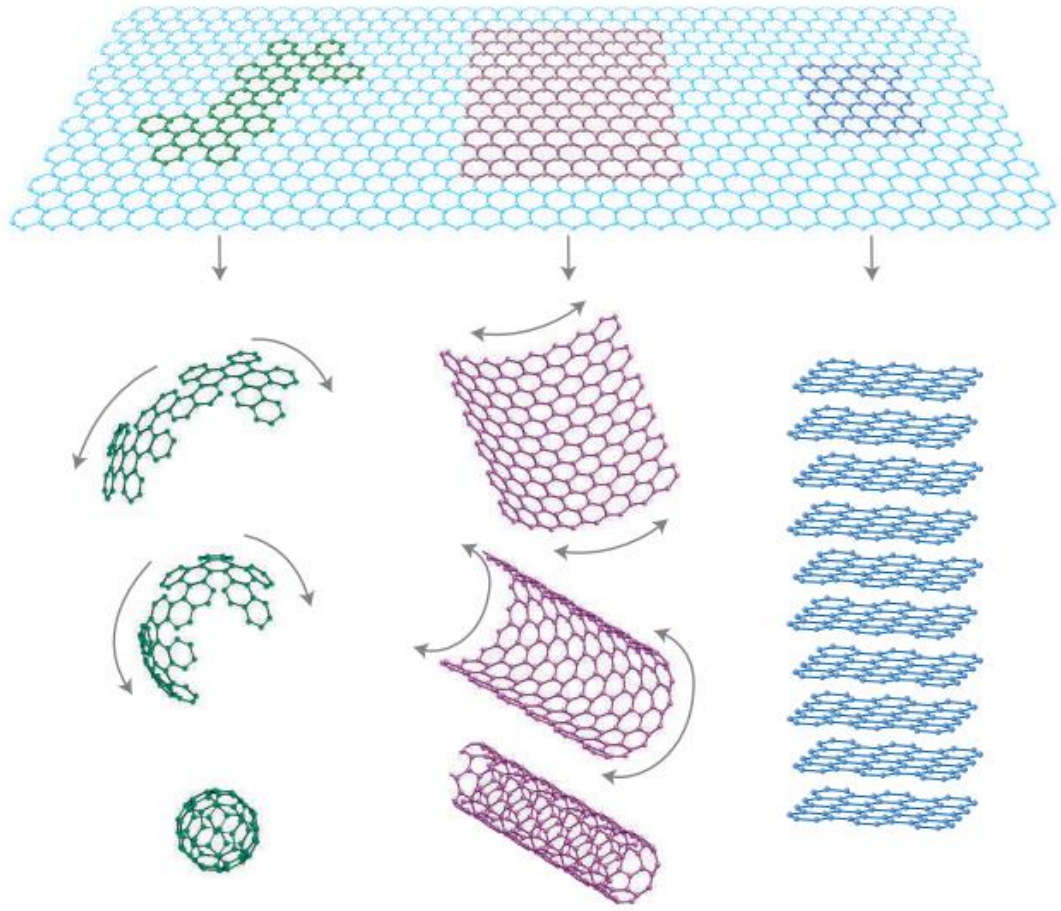

Figure 1. Schematic of graphitic forms. Graphene is a 2D building material for carbon materials of all other dimensionalities. It can be wrapped up into 0D buckyballs, rolled into 1D nanotubes or stacked into 3D graphite [30].

Carbon nanotubes can be thought of as rolled up sheets of graphene [31] as shown in Figure 1. SWCNTs are composed of a single tube of graphene, whereas MWCNTs are composed of two or more concentric tubes of graphene fitted one inside the other. The lengths of the CNTs are typically in the nanometer to micrometer range while the diameter varies from a less than one to several tens of nanometers.

Since carbon nanotubes cannot be described by conventional crystallography methods of three dimensional solids [25], new methods of describing the structure and symmetry of nanotubes have been developed by Dresselhaus et al. [32, 33]. In this

methodology the structure of nanotubes are described in terms of a vector (C), joining two equivalent points in the graphene lattice that describes the chirality of a specific CNT as shown in equation (1).

$$C = na_1 + ma_2 \; where \;\; n \geq m \qquad (1)$$

Where n and m are a pair of integers that represent a possible tube structure and a_1 and a_2 are the unit cell base vectors of the graphene sheet.

A sheet of graphene can be rolled up to obtain tubes of different chiralities or helicities known as armchair, zig-zag and chiral. These structures are schematically represented in Figure 2. If the value of (n-m) is equal to zero, then the tube is metallic (armchair) with a band gap energy of 0 eV. If the value of (n-m) is a multiple of 3, then the tube is semi-metallic (zig-zag) with a band gap energy in the range of meV and if the value of (n-m) is not a multiple of 3, the tube is semi-conducting (chiral) with a band gap energy of 0.5 to 1 eV [34]. For the case of SWNTs, the chirality sets the electrical, mechanical and other properties of CNTs [31, 32]. For MWCNTs, the chiralities of each concentric nanotube are usually different, making it impossible to predict the physical properties of these tubes according to their chiralities [23].

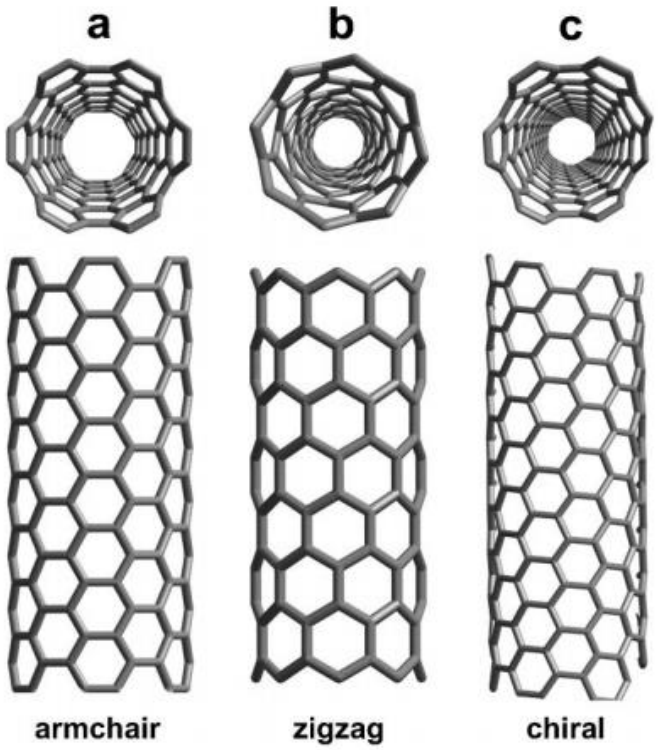

Figure 2. Structure of carbon nanotubes: a) armchair, b) zigzag nanotubes and c) chiral nanotubes (Reproduced from reference [35])

The diameter of a single tube can be calculated from the n and m indexes as indicated in equation (2) [23]:

$$d = \frac{a_{c-c}\sqrt{3(n^2+mn+m^2)}}{\pi} \qquad (2)$$

Where $a_{c\text{-}c}$ is the carbon bond length (or 1.42 Å). For the case of MWCNTs the outside tube is the one that determines the overall diameter.

The orientation of the hexagons in a carbon nanotube, also known as chiral angle (θ), can also be calculated from the n and m indexes as presented in equation (3) [23]:

$$\theta = \tan^{-1}\left(\frac{\sqrt{3m}}{2n+m}\right) \qquad (3)$$

The chiral angle varies from 0° (zig-zag) to 30° (armchair).

To calculate the number of carbon atoms (N) from a flat sheet of graphene we can use a version of the Euler's rule [36] as shown in equation (4):

$$N = 6n^2 \qquad (4)$$

Where n is the radius in hexagons.

2.1.3 Properties of carbon nanotubes

Investigations with carbon nanotubes have shown that CNTs have a combination of exceptionally unique properties, such as very high mechanical properties making them one of the strongest material known to mankind, and superior thermal and electrical properties [26]. Much of these outstanding properties are due to its special structure composed entirely of sp^2 carbon–carbon bonds which is stronger than the sp^3 carbon-carbon bonds found in other allotropes of carbon such as diamond [37].

All these properties combine in a single material together with their high strength-to-weight and modulus-to-weight ratio [38] makes CNTs one of the most promising reinforcement materials. Table 1, displays some important properties of CNTs.

Table 1. Theoretical and experimental properties of carbon nanotubes. (Modified from [39])

Property	Value
Specific gravity	0.8 g/cm^3 for SWCNTs and 1.8 g/cm^3 for MWCNTs (Depends on diameter and number of walls)
Elastic modulus	~ 1 TPa for SWCNT and 0.3–1 TPa for MWCNT
Strength	50–500 GPa for SWCNT and 10–60 GPa for MWCNT
Resistivity	5–50 μΩ cm
Thermal conductivity	3000 W m^{-1} K^{-1} (theoretical)
Magnetic susceptibility	22 x 10^{6}EMU/g (perpendicular with plane), 0.5 x 10^6 EMU/g (parallel with plane)
Thermal expansion	Negligible (theoretical)
Thermal stability	>500 °C (in air); 2800 °C (in vacuum) (Depends on diameter)
Specific surface area	10–20 m^2/g (Depends strongly on nanotube type, diameter and number of walls)

2.1.3.1 Electrical properties of nanotubes in composites

The electronic properties of carbon nanotubes are a function of both tube structure (chirality) and diameter [25]. Tube structure refers to the chirality of the only wall for SWCNTs and the outer wall for MWCNTs. The tube structure of SWCNTs can make the tubes either metallic or semiconducting while the tube structure of the outer shell of MWCNTs are predominantly metallic [40].

An enhancement of several orders of magnitude in conductivity is commonly achieved with low CNT concentrations for several composites including polymer nanocomposites; typically less than 5 wt % for the majority of polymer/CNT composites [41]. As the CNT concentration increases, the nanocomposites undergo a transition from electrically insulative to conductive as a result of CNTs forming a percolated network that provides a continuous electron path [42]. This critical concentration of CNTs forming an interconnected network and where a sharp jump in the electrical conductivity starts to occur is known as percolation threshold.

The aspect ratio (L/D) of CNTs is a fundamental parameter in the percolation threshold of composites. According to the classical percolation theory for rigid rods, the volume percolation threshold (φ_p), is inversely proportional to the inverse of the aspect ratio as shown in equation (5) [34]:

$$\varphi_p = \frac{D}{2L} \qquad (5)$$

The above equation predicts the theoretical percolation threshold and usually provides values in the range of 0.005-0.0015 due to the fact that most of the aspect ratios reported for most composites are in the range of 100-1000 [12]. However, in most cases φ_p will be above the ones given by equation (5) because non-random dispersion [43] and the fact that nanotubes are not rigid rods will affect the percolation threshold. Nanotube long-axis alignment can also play a role on the percolation threshold of the composites [44, 45]. The measurement of the electrical and/or oscillatory rheological properties is the way most often used to detect the percolation composition and is related to the dispersion of the CNTs in the host matrix [37, 46].

2.1.3.2 Mechanical properties

The mechanical properties of CNTs have been reported as to exceed those of any existing materials [47, 48] with Young's Modulus and tensile strength of the order of ~ 1 Tpa and 50-200 GPa, respectively [48] (see also Table 1) and has stimulated a growing interest in using CNTs as reinforcement materials.

In general, typical mechanical properties such as strain at break and Young's Modulus, increase with CNT concentration and dispersion [13]. However, there is usually a concentration, typically ~1 %, where usually no more reinforcement effect is appreciable [49, 50]. Two main requisites are necessary for achieving good mechanical properties when using CNTs as a filler: 1) Good compatibilization between the CNTs and the polymer matrix as to maximize the load transfer and 2) Good dispersion of the CNTs in the host matrix [37].

2.1.3.3 Dispersion and properties

Dispersion is the process of individualization of CNTs from bundles and entanglements within a matrix [51]. In large scale production of MWCNTs, the formation of bundles and entanglements formed by thousands of individual nanotubes during synthesis and purification is virtually unavoidable. These kinds of bundles and agglomerates have a profound effect on properties and will diminish mechanical and electrical properties of composites as compared with theoretical predictions related to individual CNT. Removing tubes from bundles are beneficial to achieve low percolation thresholds and high mechanical properties. Therefore, how to remove CNTs from bundles is the most significant challenge when trying to incorporate CNTs into a polymer matrix and can help gain a better insight on the structure-property relationships to improve material properties and processing conditions [52] .

Dispersion of CNTs inside a polymer matrix in melt mixing is affected by how well the chains of the host polymer infiltrate into the CNT aggregates during melt mixing. Infiltration enables cracking and erosion of aggregates and pulls CNTs apart [53]. In terms of electrical properties, the overall goal of a good dispersion is to connect CNTs so that they form a network which is usually done by separating individual tubes from each other and allowing some reagglomeration to occur. Dispersion of CNTs is so important that it has been shown that polymer nanocomposites prepared with CNTs with similar aspect ratios and characteristics can have very different percolation thresholds only on the basis of the dispersion states of the CNTs in the polymer matrix [46, 54].

Several direct or indirect methods are used to evaluate CNT dispersion in a polymer matrix. Among the direct methods, microscopic techniques such as scanning electron microscopy (SEM), optical microscopy (OM), atomic force microscopy (AFM)

etc. are the most important ones [12, 51, 55]. The indirect methods, on the other hand, usually include the measurement of the electrical conductivity [12] of the composite which provides insight into the percolated network structure of CNTs, due to the fact that in order for the composite to be conductive it must create a network to conduct the electrons. These indirect methods have the advantage of also providing information about the charge transfer mechanism (tunneling/physical touching) [12] and act as a measurement for the content and dispersion state of CNTs [56].

2.2 Carbon nanotube pre-treatment methods

All commercial forms of carbon nanotubes are synthesized with a catalyst support (usually silica) and a catalyst. In the purification step, carbon nanotubes are washed in acidic solutions to remove the catalyst and its support; further washing with water removes the acid along with the byproducts. For easier handling and storage and also for preparing polymer nanocomposites in large scale, it is more convenient to have the CNTs in a dry state and hence usually drying methods are carried out to yield the CNTs in a powder form. Thermal treatment is also useful for improving the CNT surface as well as removing non-nanotube carbonaceous materials [57] and thus a combination of acid treatments together with thermal treatments is usually encountered in industry. The requirement of an acid wash means that the nanotubes must be dried in order to make a powder. Dispersion of CNTs have been reported to improve when an acid wash is followed by the conventional oven drying (OD) or the less common freeze drying (FD) [12, 15, 19, 56-61] when compared with nanotubes powders with no previous acid treatment. Oven drying yields a more compact powder due to capillary forces that pack

and stick the nanotubes and make CNTs more prone to form aggregates than in freeze drying [60]. In freeze drying (FD), the dispersed CNT in water solution is quickly frozen (temperatures of around -20°C are usually used [56, 59]) to avoid any flocking and then the ice solution is put under vacuum [62]. The water is sublimated, giving rise to a less compact and less dense CNT powder. FD methods have the additional advantage to present fixation in situ [59, 63], which has been exploited to prepare CNT aerogels [63], CNT solid foams [64, 65], and even the world's lightest material up to date [66].

The effect of drying in the dispersion and further in the properties of nanocomposites, has been until recently, largely overlooked or not recognized in the literature and very few studies have been done to compare the dispersion state and different properties of nanocomposites for the case of OD and FD methods [15, 19, 56-61, 67]. Strictly speaking there are at least seven different approaches in which the drying methods can be part of the preparation of nanocomposites:

1) Dry nanotubes by any of the two drying methods and then melt mix the dried nanotubes directly with polymer.

2) Dry nanotubes by any drying method and then add them and disperse them (e.g. by stirring or sonication) in a solvent in which a polymer is already dissolved. Evaporate the solvent to obtain the polymer nanocomposite in a solid form.

3) Dry nanotubes by any drying method and then disperse them (e.g. by stirring or sonication) in an organic solvent or water in which a polymer will be later add and dissolved. Evaporate the solvent to obtain the polymer nanocomposite in a solid form.

4) Dry nanotubes by any drying method and then disperse them (e.g. by stirring or sonication) in an organic solvent or water. In a separate container dissolved a polymer

in the same solvent. Mix together the polymer and nanotubes in a third container. Evaporate the solvent to obtain the polymer nanocomposite in a solid form.

5) Prepare the polymer nanocomposite by 2), 3) or 4) with initially undried nanotubes and then dry the nanocomposite as a whole by any of the two drying methods.

6) Dry nanotubes by any drying method and then disperse them (e.g. by stirring or sonication) in an organic solvent or water. Subsequently, add the dispersed nanotubes to a low viscosity thermoset and evaporate the solvent to obtain a viscous liquid mixture. Finally cure the resin to obtain a solid polymer nanocomposite.

7) Dry nanotubes by any drying method and then add them directly into a low viscosity thermoset. Finally cure the resin to obtain a solid polymer nanocomposite.

The above are based on the most common nanocomposite preparation methods and are by no means the only ones possible. Approach 1 is based on melt processing where the polymer is softened and melted by heating and then mixed with the carbon nanotubes while applying a shear stress. This approach is suitable for most thermoplastic polymers and is the approach used in this work. Approaches from 2 to 5, are based on solution mixing processing (also known as solution blending), where the polymer and the CNTs are mixed in a solvent under agitation, facilitating the disaggregation and disentanglements of CNTs while controlling the evaporation of the solvent to obtain a composite in a dry state. This approach is restricted by the solubility of the polymer and suitable for polymers with high viscosities that cannot be prepared by melt processing.

Although approaches 2, 3 and 4 seem similar, the order in which the polymer and nanotubes are mixed can alter the final properties. For instance, unlike approach 2, the dispersion of nanotubes in approaches 3 and 4 are performed separately from the

dissolution of the polymer due to the fact that sonication can reduce the molecular weight of the polymer and also to avoid the rise in viscosity upon the addition of the polymer that can reduce the disaggregation of the nanotubes by sonication or other means [23]. Mixing dried nanotubes (instead of undried nanotubes) with a polymer in any of these three approaches is not very common due to the fact that the nanotubes will be submitted to a wet process again and the effect of the previous applied drying method could be lessen or lost. Approaches 6 and 7 are based on the processing of nanocomposites where the polymer is a thermoset and the CNTs are dispersed in a liquid epoxy resin and then cured by chemical (hardeners such as triethylene tetramine) or physical methods (pressure or temperature). A key issue in all the approaches, except approach 1, is the rate at which the solvent is evaporated. The faster the solvent evaporates the less time there is for carbon nanotubes to reaggreate [68]. Similarly, other ways exist in which the drying methods can be used in the preparation of nanocomposites; for example, in the mixing of nanotubes with polymer powders.

Most of the literature on comparing the effect of both freeze drying and oven drying in the dispersion of CNTs or the properties of polymer nanocomposites, focuses on fiber/epoxy composites [56, 58, 59, 61] where the CNTs were mixed with a low viscosity liquid (Approach 7) or in cases where a nanocomposite has to be prepared by a solution mixing process due to the high melt viscosities of the polymer used (e.g. UHMWPE/CNT composites) [15, 56, 58, 59, 61, 67]. In the latter case, the composite must be dried in order to compression mold samples and hence the nanocomposites are freeze dried or oven dried as a whole (Approach 5). Only three papers were found that apply the freeze drying or oven drying process directly to the CNTs in order to have a less compact and

better dispersed pristine CNT powder, before incorporating them into the polymer matrix by melt processing [19, 57, 60] (Approach 1).

Sung et al. [19], conducted studies on the rheological and electrical properties of PC/MWCNTs with MWCNTs treated with H_2O_2 and then dried by thermal or freeze drying methods. The electrical conductivity was higher for the H_2O_2-treated MWCNTs with freeze drying than with the oven drying method, as a direct effect of a better dispersion. An improvement in electrical and mechanical properties, as well as the dispersion state when the freeze drying method is compared with the oven drying method is the common observation made in the literature [15, 19, 56, 58-61, 67]. Park et al. [57] pre-treated MWCNTs with two methods: 1) acid treatment and subsequently freeze dried the MWCNTs and 2) oven dried pristine MWCNTs at 500°C for one hour. This publication is the only scientific paper found where OD samples are better dispersed and present better electrical conductivities than FD samples. However, this study is not a true comparison of the two methods, because the CNTs were not acid treated in both drying methods and also because the rather harsh temperature (500°C) used in the oven drying process can alter the chemical nature of the tubes. Additionally, the acid treatment used in the freeze drying method might provide functional groups on the structure of the CNTs and make the tubes non-conductive, as usually is the case when concentrated acid treatments are used.

2.3 Carbon nanotube length, density and powder size

Important parameters commonly encountered that can significantly affect dispersion, electrical and mechanical properties are carbon nanotube length and the way

in which composites are prepared [69-74]. Other parameters such as different synthesis methods [75], CNT type (MWCNT or SWCNT), CNT waviness [76], and the morphology of the aggregates [16, 77] are also known to impact the dispersion and properties of the polymer composites.

In the case of CNT length, typically carbon nanotube length reduction is unwanted and often occurs during mixing of nanotubes with the composite. Most commercial MWCNTs have an average length of about 1 micron. [78]. Recent work with longer tubes, including some having an average length of 4.5 microns [10], has shown that polymer degradation can be enhanced with longer tubes, and that the longer nanotubes were broken to a much larger extent (a factor of ~2 for the 1 micron tubes and a factor of ~5 for the 4.5 micron tubes). These two factors tend to blunt the impact of longer tubes on properties. In this regard, a key issue is to understand better processing conditions that can be used to minimize both of these effects; however another option is to grow longer tubes and then purposefully break them before mixing with the polymer. This approach may seem counterintuitive, however, yield (pounds of nanotube/pounds of catalyst) is a critical economic driver of nanotube production and longer tubes often correspond to higher yields. Shortening CNTs in this manner can reduce interactions between CNTs improving the dispersability in the matrix [79], which is directly linked with the composite properties.

A property correlated with the dispersion of CNTs in a polymeric matrix and a sub-product of the drying method chosen is bulk density [16, 53, 76, 80, 81]. Significant differences exist depending on the process conditions (temperature, type of catalyst etc) [82]. Morcom et al. [16], studied the effect of different CNTs properties on the degree of

dispersion and reinforcement of high density polyethylene (HDPE). Regarding bulk density, the authors concluded that a low bulk density provide an easier path for a polymer to infiltrate between the nanotubes due to higher spacing between nanotubes, which in turn creates a better dispersion of the CNTs. Morcom et al., also discussed the effect of aspect ratio (length/diameter) on the yield strength, concluding that the yield strength is higher for the composites with greater aspect ratios. In this and many other studies, the difference between as-received average length of CNTs and breakage of tubes during the composite preparation is usually not taken into consideration [83]. Obviously, the nanotube length distribution in the composite is relevant for properties of the composite [38, 79, 83, 84].

Powder size or granular size is related to the bulk density. Large particle sizes normally lead to higher bulk densities. In this work, the starting powder size will be also considered to evaluate the role of density in the dispersability of MWCNTs. No scientific work was found studying the direct effect of powder size on the dispersion or properties of polymer based composites.

Chapter 3: Methodology and experimental methods

3.1 Materials

The polymer used in this study was polycarbonate (Makrolon® 2600, Bayer MaterialScience AG, Leverkusen, Germany) having a medium viscosity which correspond to a melt flow rate of 12 cm^3/10 min at 300 °C/1.2 kg according to the manufacturer. Fourteen MWCNTs (SouthWest NanoTechnologies (SWeNT), Norman, OK), all with the same characteristics but with two different pre-treatment (e.g. OD and FD) methods, different powder sizes, densities and lengths were investigated. Table 2, shows the tapped bulk density, diameter, average length, and aspect ratio, of the as-received pristine MWCNT used. All MWCNTs were produced via catalytic chemical vapor deposition (CCVD), using a CoMoCAT® catalyst and a fluidized bed reactor that enables optimal control of CNT structure and purity. MWCNT samples were purified by the manufacturer by dissolving the residual catalyst particles in the presence of an aqueous solution containing 25 v% of hydrofluoric acid at room temperature for 3 hours. The CNT slurry is subsequently filtered using a plastic Buchner filter and then the paste formed is washed with deionized hot water to achieve a neutral pH. The carbon nanotube material is subsequently dried in a conventional oven at 120°C, or in a freeze drier equipment at liquid nitrogen temperature (-210 to -195 °C) under vacuum, to obtain a fine powder. The purified MWCNTs are finally submitted to mechanical methods developed by SWeNT to reduce CNT length.

3.2 Composite preparation

Composites of PC/MWCNT were melt-mixed using a 5 cm^3 DSM twin screw micro-compounder at a mixing temperature of 280°C, a mixing time of 5 min, and a mixing speed of 200 rpm with a continuous flow of nitrogen to reduce polymer degradation during mixing, as done in our previous work [10, 78]. The total amount of processed material was 4.2 g. Before the mixing experiments, the polymer were dried at 80 °C under vacuum overnight and then premixed with the as received CNTs with a fixed speed vortex mixer. Pellets obtained from extruded strands were compressed molded in a Carver Laboratory Press into films with a thickness ranging from 0.3 to 0.5 mm using a pressing temperature of 280°C and a pressure of 45 kN.

3.3 Composite Characterization

3.3.1 Nanotube length distribution

To measure tube length after mixing with a polymer, 1 mg of the composites were introduced in a glass flask containing 10 ml of chloroform at room temperature leading to a concentration of 0.1g/l and then left without any further treatment for 1h, as described elsewhere [83]. In the case of pristine MWCNTs, nanotubes were dispersed in chloroform as well. After a treatment for 3 min in an ultrasonic bath (Cole-Parmer, frequency 42kHz, ultrasonic power 70W), which is assumed not to shorten nanotube length significantly [83], a drop of the solution was placed on a silicon wafer and the samples were placed in the fume hood until the solvent evaporates. The silicon wafer, was then place in a SEM holder and the MWCNTs lengths were measured with the free software Image-J on approximately 100 tubes not touching edges and completely visible

from begin to end. The distributions parameters x10, x50, and x90 were calculated to further characterize the length distribution of CNTs, indicating that 10, 50, and 90% of the nanotubes are smaller than the given value.

In order to evaluate the morphology of the primary agglomerates before melt mixing, the different MWCNTs in a powder form were observed by SEM. A Zeiss Neon 40EsB SEM was used in all cases described here and average values were reported.

3.3.2 Electrical resistivity

Electrical resistivities (ρ) were measured at room temperature following the ASTM D 257 for insulating materials (resistivities > 1 x 10^7 Ohm-cm) using an Agilent 4339B High Resistance Meter with an Agilent 16008B resistivity cell. Compression molded films were tested at least 3 times on each face surface and the average resistivity value was reported. Four-point probe resistivity measurement (Copper electrodes attached using silver conductive epoxy with a distance of 10 mm between each electrode) was used to measure resistance for moderately conductive materials (resistivities < 1 x 10^7 Ohm-cm), using a Keithley 2000 Multimeter. Six strips (30x3x0.5 mm3) cut from the compression molded samples were measured and the average resistivity was obtained according to Equation (6).

$$\sigma = \frac{1}{\sigma} = \frac{Rab}{c} \qquad (6)$$

σ is the conductivity, R is the resistance, *a* is the film thickness, *b* is the width and c is the length of the film. The percolation threshold will be determined numerically by fitting the experimental data to Equation (7).

$$\sigma = B(p - p_c)^t \qquad for\ p > p_c \qquad (7)$$

p is the MWCNT weight percentage (p), *B* is a proportionality constant, *pc* is the electrical percolation threshold, and *t* is the critical exponent.

All electrical measurements were conducted to as received MWCNTs and composites without drying. An additional experiment of nominally dry the as-received pre-treated MWCNTs at 120 °C under vacuum overnight to remove water, was performed with selected nanotubes to evaluate the effect of this ubiquitous step on the electrical properties and the percolation threshold.

3.3.3 Mechanical properties

Tensile tests were performed on a United STM-2K tensile tester at 1.2 cm/minute. Samples were cut from compression molded films using an ASTM-D-1708 expulsion die on a manual expulsion press, both from Dewes-Gumbs. Data was collected from at least 5 samples.

3.3.4 Macro dispersion state

Compression molded sheets were imaged using a Zeiss ApoTome equipped with a 40x/0.7NA dry objective, a 0.9 NA dry condenser and an Axiocam Mrm CCD camera. The samples were imaged via a transmitted bright field focus series forming a bright field z-stack to generate a 3D reconstruction of the volume of the intact sample. Each Z-Stack projection contains normally more than 3000 agglomerates. This reconstruction from the series of collected images along the optical axis (Z-axis) was used to quantify the agglomerate area and agglomerate volume distributions of the samples.

The methodology for agglomerate volume distribution followed two steps:

1) Image analysis, where the images are processed with a bandpass filter (to remove the out of focus component and camera noise), binarized (such that agglomerates had an intensity of 1 while the polymer matrix an intensity of 0) and agglomerate characteristic sizes in two dimensions (diameters, lengths, aspect ratios etc.) are calculated.

2) Due to the insufficient information on the agglomerate dimensions along the optical axis, mainly because of a refractive index mismatch between the sample and the objective that increases spherical aberration [85] and the low NA of the objective used, the MWCNT agglomerate volumes were calculated by fitting a lateral box to each agglomerate and averaging both axes to get an estimate of the agglomerate diameter and then assuming the agglomerates to be spheres. This shape assumption is the most common assumption in stereology (the science of inferring 3D distributions from 2D information) and is the closest simple geometrical volume that can represent agglomerates of random sizes and at random positions.

Since melt mixing processing will presumably generate a random shearing of the MWCNTs inside the polymer matrix [86], the methodology employed to calculate the volume distribution will be validated if it presents a log-normal distribution [87, 88].

In the case of the agglomerate area, the MWCNT agglomerate area distribution was calculated from the profile particles in the X and Y directions. Agglomerate size distribution were used in this methodology to determine the area ratio (AA) and average agglomerate area from the images using the image analysis software ImageJ by calculating the ratio of MWCNT agglomerate area to the total area of the image. Only agglomerates with circle-equivalent diameters larger than 5 μm were considered as agglomerates as according to the ISO 18553 [89].

Samples at 0.2 wt% were selected in both cases because this low concentration allowed MWCNT agglomerates to be seen along the Z-axis in a matrix with a large refractive index (RI) as polycarbonate (RI is approximately 1.584).

3.3.5 Micro dispersion state

SEM micrographs were collected with Zeiss Neon 40EsB SEM to evaluate the state of dispersion of the CNTs inside the polymer matrix in the micro scale of selected concentrations.

3.3.6 Thermal Analysis

Thermogravimetric analysis (TGA) was used to validate the chemistry, dispersion and purity of selected oven and freeze dried MWCNTs using a Netzsch STA 449 F1 Jupiter TGA. Approximately 10–20 mg of MWCNTs was loaded in the TGA and heated

to 100 °C and held for 30 min to remove moisture, followed by heating up to 800 °C at rates of 1 K/min and 3 K/min under a gas mixture of 10 ml helium and 40 ml air, and then being held at 800 °C for 30 min to allow the nanotubes to completely degrade.

Chapter 4: Results and discussion

4.1 MWCNT characteristics

Table 2 shows the tapped density, average length, diameter and aspect ratio of all as-received MWCNTs used in this study. All samples were named after the aspect ratio (AR) of the as received nanotubes and the pre-treatment method used. UNP stands for unpurified samples that were not purified and dried by any method. Additionally, a notation like "<30, 2.2-1.4" mm means that the MWCNTs were sieved in a series of sieves of mesh diameter of less than 30 mm and the powder diameter of the MWCNTs are in the range of 2.2 to 1.4 mm. MWCNTs with this notation were sieved to evaluate the role of particle diameter in the dispersion. The rest of the MWCNTs have the same powder size.

Table 2. Density, average length, diameter and aspect ratio of as-received MWCNTs

Samples	Tapped density (Kg/m^3)	Average Length (nm)	Diameter (nm)	Aspect ratio
AR 107 FD	73	1020	9.5	107
AR 130 FD	60.4	1300	10	130
AR 227 FD	45.34	2160	9.5	227
AR 90 OD	95	900	10	90
AR 103 OD	106.6	980	9.5	103
AR 122 OD	98	1160	9.5	122
AR 207 OD	112	2068	10	207
AR 95 OD <30, 3.2-2.2 mm	123.2	900	9.5	95
AR 158 OD <30, 2.2-1.4 mm	143.5	1500	9.5	158
AR 116 OD <30, 1.4-0.85 mm	121.4	1100	9.5	116
AR 95 OD <30, < 0.850 mm	105	900	9.5	95
AR 82 UNP	53.2	820	10	82
AR 94 UNP	65.7	940	10	94
AR 107 UNP	53	1070	10	107

Table 2 also shows that the average aspect ratios were between 82 and 227, which is in the range of most commercial MWCNTs [10]. Additionally, unpurified samples have the lowest densities which normally are beneficial for the dispersion of CNTs inside a polymer matrix. Unfortunately, CNTs that are not purified usually contain high amounts of catalyst and support as well as carbonaceous impurities that are detrimental to the mechanical and electrical properties. All freeze-dried MWCNTs had lower densities (the range was 45.34-73 Kg/m^3) than the oven-dried MWCNTs (the range was 90.6-143.5 Kg/m^3).

4.2 Length distribution

Figure 3, shows an example of two SEM micrographs to measure CNT lengths. The pictures to the left are the micrographs obtained with the SEM while the pictures to the right show how individual CNTs were bordered with the help of the software Image J to quantify the individual lengths, once the pictures were scaled with the scale bar. This process was repeated with several pictures until obtaining 100 individual CNT lengths to obtain the average CNT length and statistical distribution parameters.

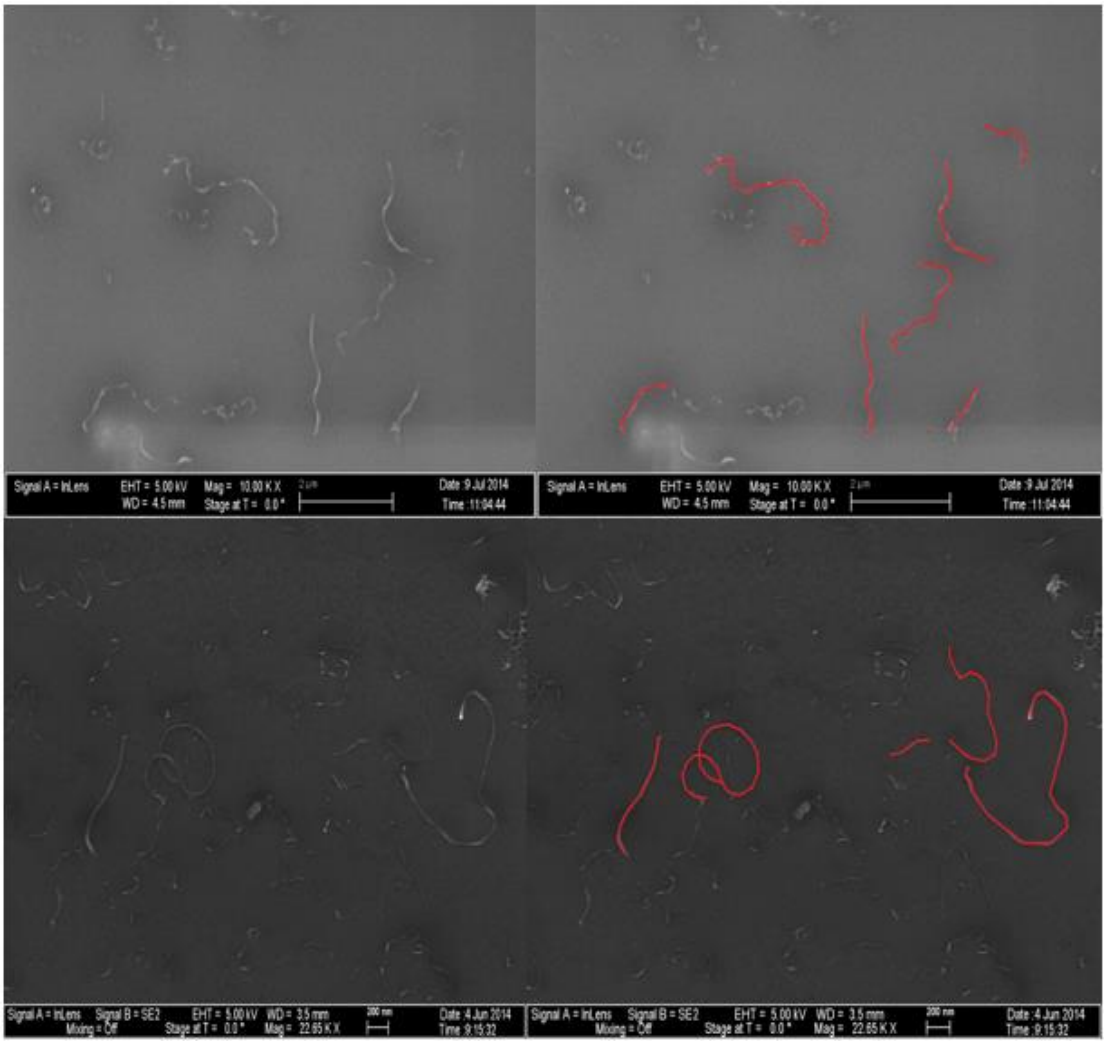

Figure 3. SEM micrographs showing the process to measure the MWCNTs lengths.

Table 3 shows the average length, aspect ratio, average length reduction and three distribution parameters for the MWCNTs before (as-received) and after being processed in the twin screw microcompounder. For the case of as-received MWCNTs, the length of FD samples are in the range between 1020-2160 nm, for the OD samples are in the range 900-2068 nm, for the sieved nanotubes in the range of 900-1500 nm and for the unpurified MWCNTs in the range of 820-1070 nm .Since the diameter of MWCNTs are likely to remain unchanged after processing, the after processing length

is the most relevant dimension for electrical and mechanical properties as well as the dispersion state of the nanotubes.

The drying method showed to have no effect on the breakage of the tubes during melt mixing. The pair AR107 FD-AR103 OD and AR 227 FD- AR207 OD have different drying methods and similar initial lengths and they both ended up with approximately the same lengths after being melt mixed. The same trend is observed with nanotubes of different granular size as is the case of the pair AR 95 OD <30, 3.2-2.2 mm- AR 95 OD <30, < 0.850 mm with exact initial average lengths and practically exactly the same final average lengths. The only exception was the pair AR 130 FD- AR122 OD. The author does not know the source of the exceptional reduction of AR 122 OD (from 1160 to 462 nm).

Processing in the conical twin-screw under the conditions used in this work reduces the length of the MWCNTs with higher starting lengths (or aspect ratio) more than the ones with lower aspect ratio, as previously reported in our group [90]. MWCNTs with initial aspect ratios above 200 (AR 227 FD, AR 207 OD) where cut in more than half (with the exception of AR 122 OD, for the reasons mentioned above), whereas shorter tubes were cut below 50% of their original length. Reduction of initial length for MWCNT with aspect ratios below 100 was found to be below 20%.

Table 3. Aspect ratio, average length, average length reduction and distribution parameters of MWCNTs both as-received and after melt-mixing

Sample	Aspect ratio after processing	Average Length before and after processing (nm)	Length reduction (%)	x10 before and after processing (nm)	x50 before and after processing (nm)	x90 before and after processing (nm)
AR 107 FD	64	1020 - 608	40	347 - 269	885 - 562	1919 - 989
AR 130 FD	106	1300 - 1060	18	487.5 - 544	969 - 949	2290 - 1648
AR 227 FD	77	2160 - 731	66	839 - 357	1780 - 605	3975 - 1141
AR 90 OD	75	900 - 751	17	454 - 313	763 - 736	1514 - 1175
AR 103 OD	71	980 - 676	31	477 - 313	847 - 622	1598 - 1112
AR 122 OD	49	1160 - 462	60	446 - 183	912 - 377	1908 - 831
AR 207 OD	79	2068 - 793	62	673 - 545	1611 - 858	4202 - 1031
AR 95 OD <30, 3.2-2.2 mm	78	900 - 745	17	286 - 532	645 - 823	2024 - 1031
AR 158 OD <30, 2.2-1.4 mm	123	1500 - 1169	22	478 - 749	1097 - 1140	3122 - 1715
AR 116 OD <30, 1.4-0.85 mm	77	1100 - 731	34	409 - 380	960 - 681	1899 - 1111
AR 95 OD <30, < 0.850 mm	78	900 - 742	18	389 - 414	775 - 670	1527 - 1113
AR 82 UNP	71	820 - 713	13	315 - 320	727 - 639	1604 - 936
AR 94 UNP	80	940 - 804	14	326 - 389	726 - 733	1605 - 1290
AR 107 UNP	101	1070 - 1007	6	345 - 360	838 - 916	1950 - 1764

Chloroform was used because it is a suitable solvent for dissolving polycarbonate [83] and also because the dispersion of MWCNTs tends to be more stable when compare with other common solvents [91]. Table 4 shows the time needed for every sample to be completely dispersed in chloroform. Complete dispersion was evaluated qualitatively by direct observation as the point where the nanotube dispersion appears to be completely black, as exemplified in Figure 4 for several MWCNTs. Some samples needed a higher sonication time (shown in blue) to be dispersed in the solvent.

Table 4. Sonication time for all MWCNTs

Sample	Time for dispersion (min)
AR 107 FD	3
AR 130 FD	3
AR 227 FD	3
AR 90 OD	3
AR 103 OD	3
AR 122 OD	3
AR 207 OD	3
AR 95 OD <30, 3.2-2.2 mm	7
AR 158 OD <30, 2.2-1.4 mm	3
AR 116 OD <30, 1.4-0.85 mm	3
AR 95 OD <30, < 0.850 mm	3
AR 82 UNP	40
AR 94 UNP	13
AR 107 UNP	55

Only AR 95 OD <30, 3.2-2.2 mm and the three unpurified samples needed more than 3 minutes to be completely dispersed in chloroform. Not unsurprisingly, a larger powder size lengthens the time necessary to disentangle nanotubes from an agglomerate. The purification and drying methods improve the dispersability of the MWCNTs when compare with unpurified samples. Unpurified MWCNTs took the longest time to be completely dispersed in the solvent probably because the nanotubes are still attached to the support particles and the nanotubes must break, either in the middle or at the base, to become individual particles. For the unpurified MWCNTs, the length did not seem to correlate with the dispersion time.

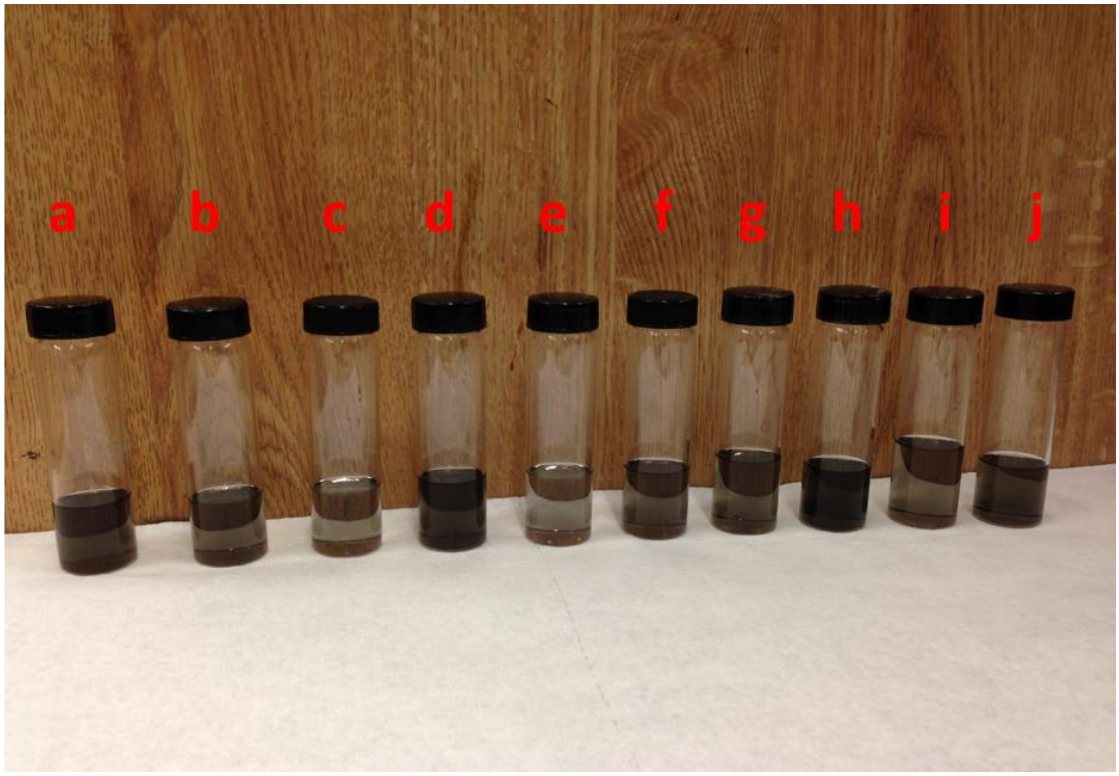

Figure 4. Qualitatively evaluation of dispersion for several of the MWCNTs used a) AR 94 UNP b) AR 107 UNP c) AR 82 UNP d) AR 90 OD e) AR 130 FD f) AR 207 OD g) AR 95 OD <30, 3.2-2.2 h)AR 158 OD <30, 2.2-1.4 i)AR 116 OD <30, 1.4-0.85 j) AR 95 OD <30, < 0.85

4.3 Electrical properties

The influence of the length, powder size, density and pre-treatment methods on the electrical percolation threshold is illustrated for selected composites in Figure 5 and for all composites in Table 5.

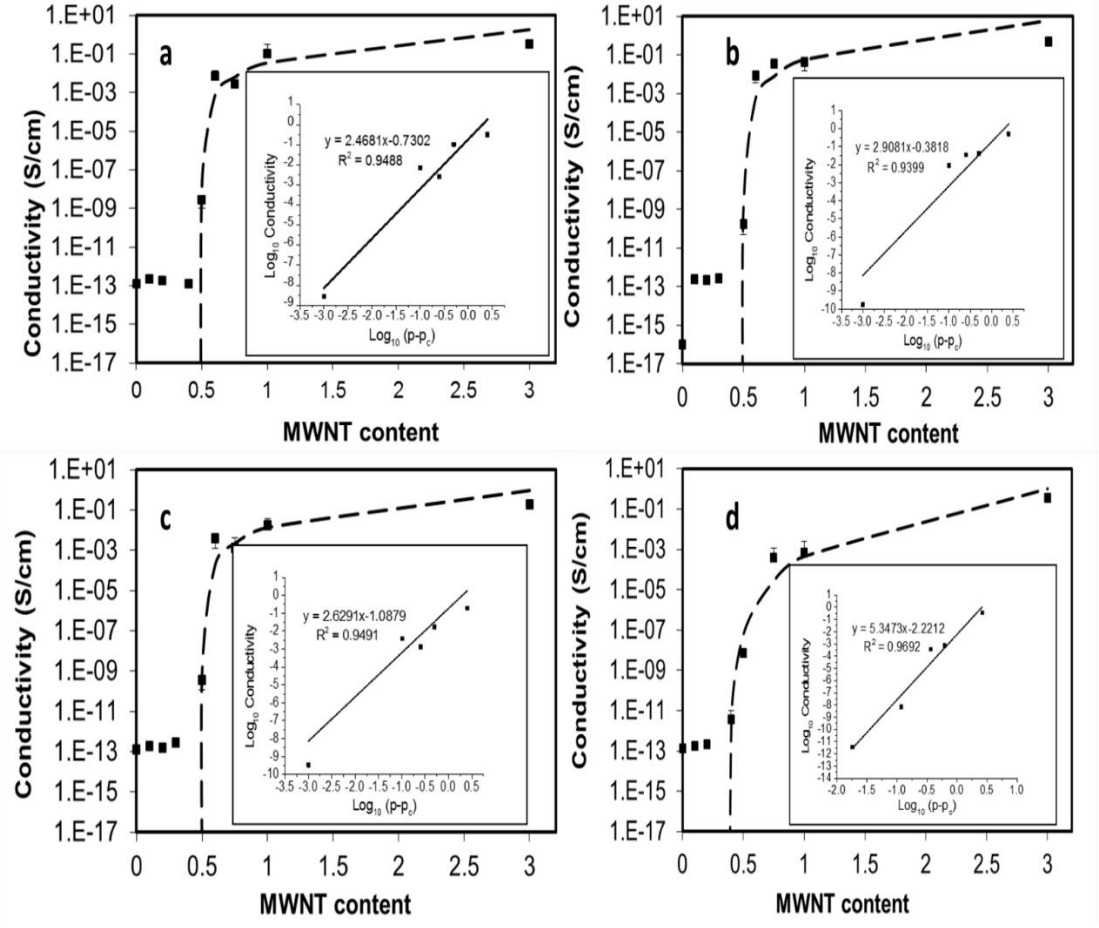

Figure 5. Volume electrical conductivity as a function of MWCNT concentration for selected composites: a) AR 207 OD b) AR 107 FD c) AR 95 OD <30, 3.2-2.2 mm d) AR 94 UNP. The inset figure represents the plot of $\log_{10}$ conductivity vs $\log_{10}$ $(p-p_c)$ where the straight line is the least-square fit for the data using equation 7.

The values fitted for the proportionality constant B, the percolation threshold p_c and the critical exponent t are shown in Table 5. Surprisingly, all oven-dried and freeze-dried samples have essentially the same percolation threshold independent of the density, after

processing length and powder size. The percolation threshold for the unpurified samples varied from 0.382 to 0.668 wt%. The longest tubes (AR 107 UNP and AR 94 UNP) presented the lowest percolation threshold and the shortest tube (AR 82 UNP) the highest percolation threshold, as expected.

Table 5. Percolation threshold and percolation parameters for all nanocomposites. The average length after processing is included to facilitate the explanations

Samples	p_c (wt%)	T	B	Average Length after processing (nm)
AR 107 FD	0.499	0.415	2.908	608
AR 130 FD	0.501	5.58E-05	6.074	1060
AR 227 FD	0.499	0.391	2.502	731
AR 90 OD	0.506	0.086	1.048	751
AR 103 OD	0.499	0.162	2.241	676
AR 122 OD	0.499	0.627	2.955	462
AR 207 OD	0.499	0.186	2.468	793
AR 95 OD <30, 3.2-2.2 mm	0.499	0.082	2.629	745
AR 158 OD <30, 2.2-1.4 mm	0.49	0.020	3.225	1169
AR 116 OD <30, 1.4-0.85 mm	0.499	0.036	2.252	731
AR 95 OD <30, < 0.850 mm	0.499	0.266	2.448	742
AR 82 UNP	0.668	0.180	0.183	713
AR 94 UNP	0.382	0.006	5.347	804
AR 107 UNP	0.400	1.44E-05	5.599	1007

The classical percolation theory predicts a dependence of the percolation threshold with the inverse of the aspect ratio but fails to take into account other key factors that may affect the conductivity such as CNT alignment, different pre-treatments methods, CNT shape and CNT waviness among others. In cases where the fillers are not homogeneously distributed and/or long tubes don't seem to enhance the percolation threshold, dispersion is a more relevant parameter [46]. The non-correlation between the aspect ratio and

percolation thresholds shown in Table 5 stems in the state of dispersion of the MWCNTs as shown in sections 4.5 and 4.6, where all the dried-CNTs presented comparable dispersions at macro and submicron scales. Likewise, it was shown that the dispersion in both scales is independent of MWCNT length. These results can be further explained from the point of view of carbon nanotube waviness (.i.e. filler bending and entanglement). Waviness has been shown to influence the percolation threshold, restricting the average contact of the nanotubes [92]. Parameters such as the static bending persistence have been used to quantitatively show that coil-like MWCNTs do not depend on the inverse of the aspect ratio [93]. Visual inspection show that the nanotube dispersion shown in Figure 3 and sections 4.5 and 4.6 are approximately similar to those shown in reference [93] to describe coil-like MWCNTs. This offers a more complete explanation because most dried-MWCNTs have lengths in the range of 608-793 nm, which are likely to present similar dispersions and percolation thresholds because of similar lengths and waviness. Longer dried-MWCNTs such as AR 130 FD and AR 158 OD <30, 2.2-1.4 mm with lengths above 1000 nm, would be expected to percolate at lower nanotube content than shorter tubes given a similar state of dispersion, but since longer tubes usually have more waviness, the interconnections between CNTs will be reduced and may give rise to a similar percolation threshold than those exhibit by short CNTs. Figure 6 shows schematically in 2 dimensions, that long and short CNTs that have similar dispersions may have similar connectedness if the tubes are curved.

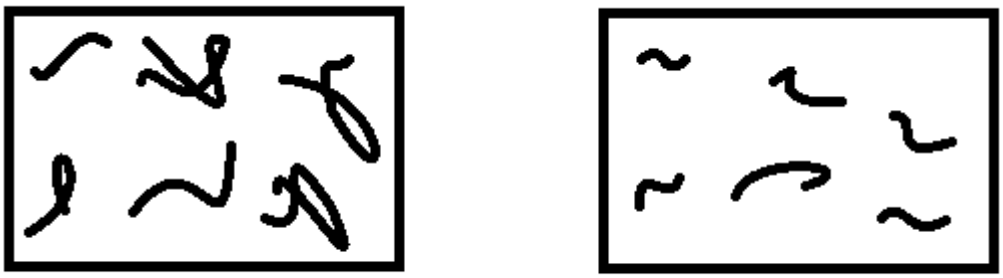

Figure 6. Schematic representation of the waviness of carbon nanotubes in two-dimensions with similar spatial distribution and connectedness. Left: Long CNTs and Right: Short CNTs

Freeze-dried MWCNTs have been shown previously to have lower percolation thresholds than oven-dried MWCNTs [15, 19, 56, 58-61, 67]. However, a lower percolation threshold is often the case when the nanotubes or composites have been submitted to an additional drying to remove functional groups or any water content gained, at any point before measuring the desired properties. To further explore the effect of an extra drying, the conductivity of composites prepared with as-received MWCNTs submitted to an additional drying prior to melt mixing were measured.

Figure 7 shows the electrical conductivity of composites prepared with pre-treated MWCNTs (by oven drying and freeze drying) submitted to an additional drying at 120°C under vacuum overnight to remove the water gained after receiving the MWCNTs and also the electrical conductivities of composites prepared with as-received MWCNTs. It is evident from Figure 7, that drying previously dried nanotubes to remove any water content gained after being received, may increase the percolation threshold of the composites.

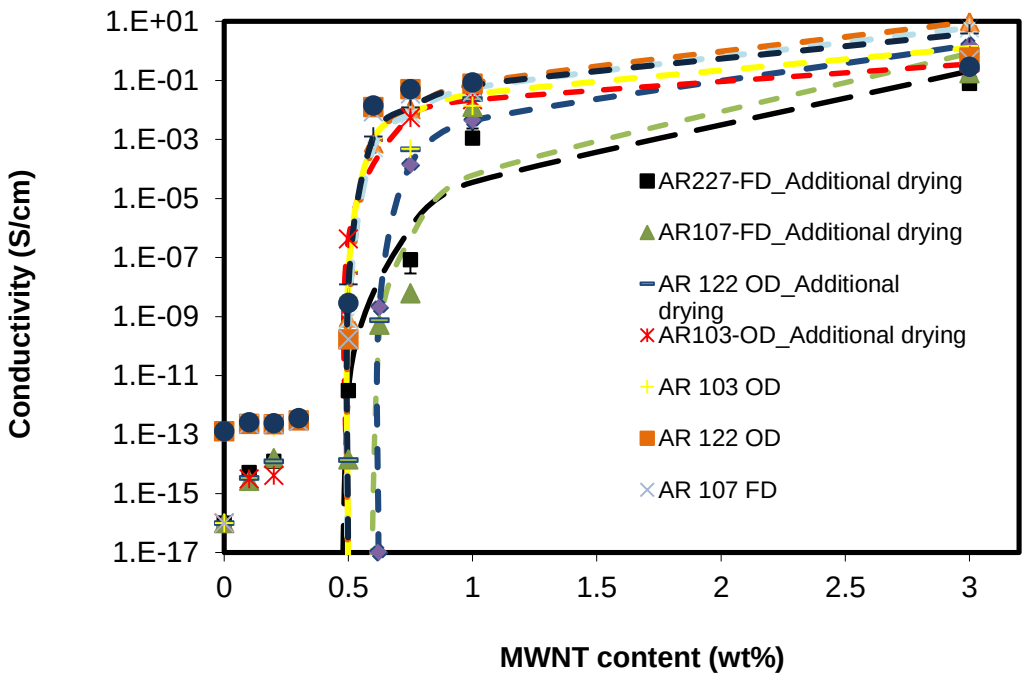

Figure 7. Comparison of the electrical conductivities of 4 composites fabricated with 4 MWCNTs with and without an additional drying

Table 6, shows the percolation threshold and percolation parameters of the samples shown in Figure 7. The fact that all the composites with nanotubes without an additional drying have the same percolation threshold makes simpler the evaluation of the effect of the additional drying. The additional drying seems to increase the percolation threshold of the composites with lower after processing lengths (AR 122 OD and AR 107 FD) independently of the drying method used. This increase does not depend on the density, as can be seen from the density data of the four composites where two of the composites that had an increased in the percolation threshold, were selected to have a higher and lower density than the other two samples (density of AR122 OD < density AR 103 OD and density of 107 FD > density AR 227 FD). The percolation of nanotubes with longer after processing lengths (AR 103 OD and AR 227 FD), are essentially not affected by the additional drying.

When drying a carbon nanotube powder in an oven or submitting it to thermal vaporization, what is essentially being done is a process of water removal and compaction of the CNT powder due to capillary forces. Despite being composed of hydrophobic graphene sheets and being unable to be dissolved in water, carbon nanotubes have been shown to absorb water vapor from the air at ambient conditions in simulation [94] and experimental studies [95-97] for both single-walled carbon nanotubes [94, 96] and multi-walled carbon nanotubes [95, 97]. Moreover, the hydrophilicity of carbon nanotubes may be enhanced by introducing surface defects [94, 98] that are usually promoted when acid treatments and drying processes have taken place, as in this study. In light of this, if a CNT powder absorbs water and the length of the nanotubes are short, the CNTs are more prone to change their existing state of dispersion to one with more entanglements and aggregates. If the length of the nanotubes are long, it is likely that they already have pre-existing entanglements and their state of dispersion and entanglements will not be modified as much. Hence the electrical properties of short nanotubes will likely change (i.e. decrease) more than the electrical properties of long tubes when both are submitted to an additional drying.

Two out of the three papers found that apply the freeze drying or oven drying process directly to the CNTs and then incorporate them into the polymer matrix by melt processing [19, 60] as done in this work, introduce an additional drying method to the nanotubes before mixing them with the polymer or to composites before the compression molding step or before measuring the properties, which may cause the reported percolation threshold to be higher than if an additional drying step was not included. These scientific works also have in common that they acid treated the MWCNTs. This is

particularly important because oven drying have been reported to break or damage MWCNTs that have been acid treated or have functional groups [19, 59, 99] even at relative low temperatures (120-150°C). So in this regard, when splitting the same type of MWCNTs to be oven dried or freeze dried, the reported decrease in electrical properties and worse dispersion for oven dried MWCNTs when compare with freeze-dried MWCNTs, may be an effect of nanotube length reduction originated during the oven drying process and/or a subsequent additional drying, instead of only the MWCNT spatial dispersion achieved by the two drying methods.

Table 6. Percolation parameters of 4 composites fabricated with 4 MWCNTs with and without an additional drying. The average length after processing is included to facilitate the explanations.

Samples	P_c	B	T	Average Length after processing (nm)
AR 103 OD_Additional drying	0.499	0.072	1.75	676
AR 122 OD_Additional drying	0.621	0.097	3.20	462
AR 107 FD_Additional drying	0.58	0.007	5.44	608
AR 227 FD_Additional drying	0.494	0.0013	4.44	731
AR 103 OD	0.499	0.162	2.24	676
AR 122 OD	0.499	0.627	2.95	462
AR 107 FD	0.499	0.415	2.91	608
AR 227 FD	0.499	0.391	2.50	731

A ubiquitous step, as removing water from the nanotubes by drying them in an oven, may then be thought as overriding the previous drying pre-treatment method applied to the nanotubes only if they are short (below 608 nm) while the previous pre-treatment of longer tubes is unaffected. Most scientific literature that compare the effect of freeze

drying and oven drying [15, 56, 58, 59, 61, 67], do not report the after processing length of the carbon nanotubes used which clearly contributes to the measured percolation threshold.

A plot of log of the electrical conductivity vs MWCNT concentration$^{-1/3}$ is presented in Figure 8 for selected nanocomposites. The fact that there is no linear variation of the log of the electrical conductivity with MWCNT concentration$^{-1/3}$, supports no tunneling mechanism in the nanocomposites [12, 100, 101]. In other words, the main cause of the formation of a CNT network and a continuous electron path is through physical touching of the carbon nanotubes. The evaluation of the nature of the charge transfer mechanism evaluated in this way only fails when there is a dynamic percolation process [12].

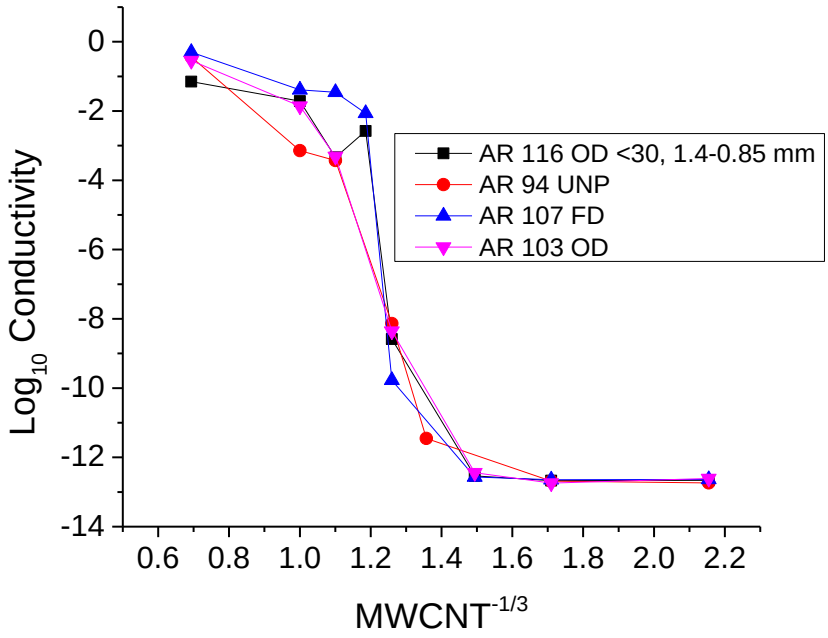

Figure 8. Graph showing the variation of log_{10} of the electrical conductivity vs MWCNT$^{-1/3}$

4.4 Mechanical properties

The effect of MWCNTs on the Young's modulus, tensile strengths and strain at break for the PC/MWCNT composites are shown in Figure 9, Figure 10 and Figure 11. Figure 9 shows that Young's modulus slightly increases with increasing MWCNT concentration when compared with pure PC as was found in our previous work for all carbon nanotube content up to 1 wt% [90]. However, for both long and short MWCNTs the Young's modulus did not correlate with MWCNT content. Also as in our previous works, [90, 102] the tensile strength did not correlate with of MWCNT concentration (Figure 10). The strain at break (Figure 11) decreases drastically when adding MWCNTs to the PC matrix [90, 102] but also does not correlate with the MWCNT concentration.

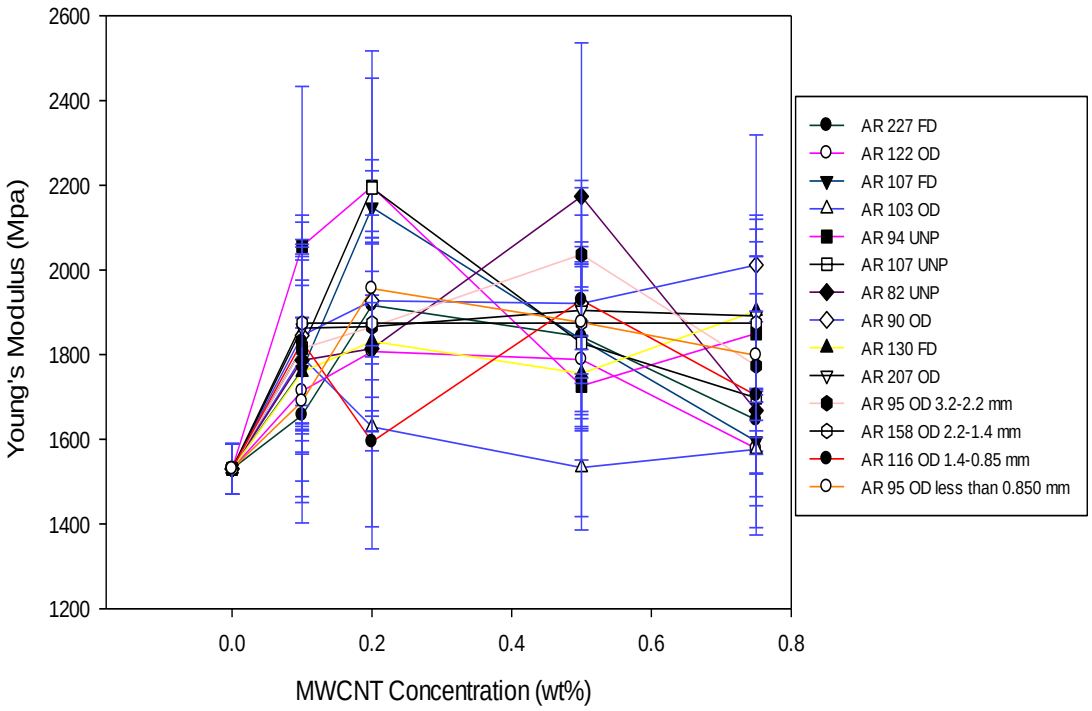

Figure 9. Young's modulus as a function of nanotube concentration for PC/MWCNT composites

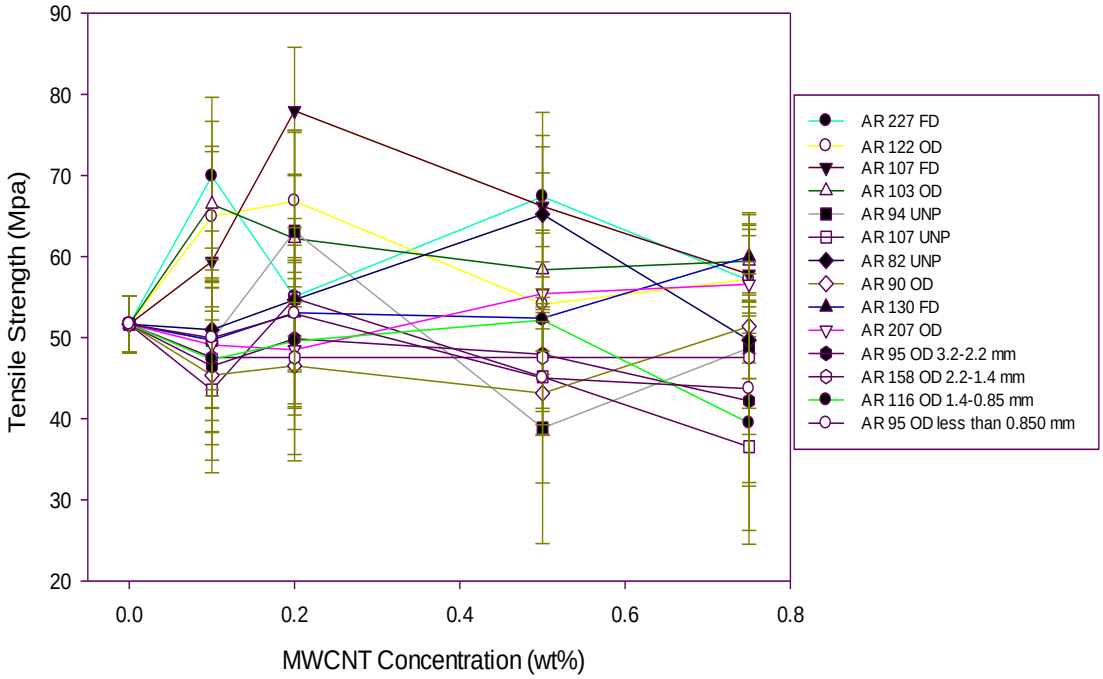

Figure 10. Tensile strength as a function of nanotube concentration for PC/MWCNT composites

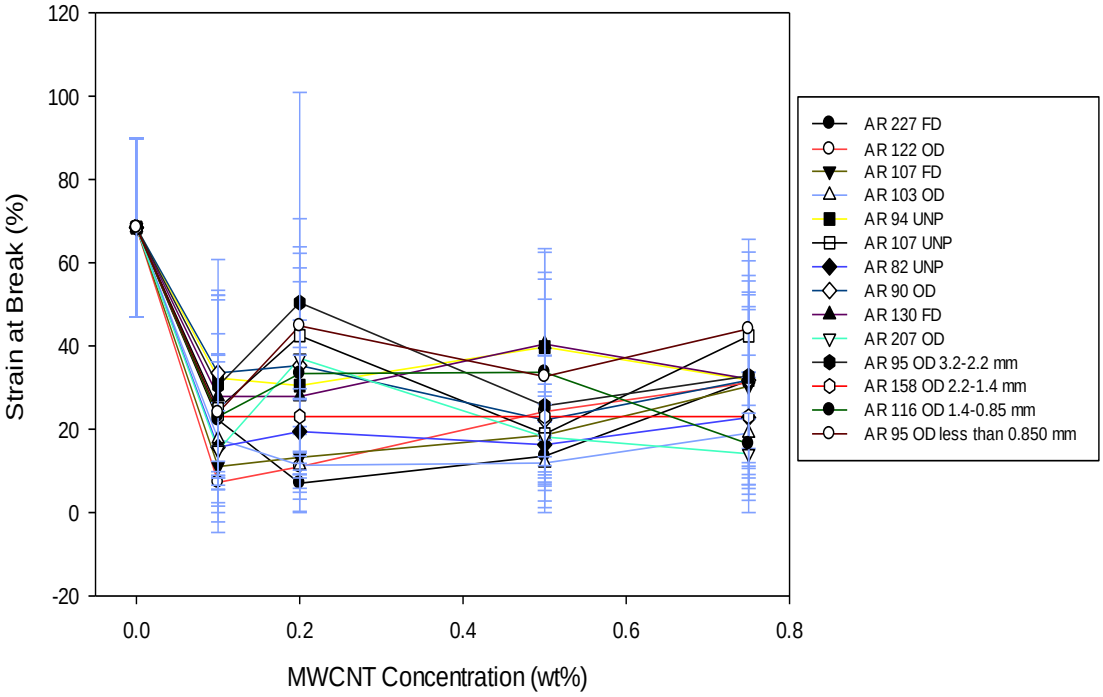

Figure 11. Strain at break as a function of nanotube concentration for PC/MWCNT composites

Figure 12 through Figure 17 show the effect of particle size and pre-treatment method on the three mechanical properties evaluated. No correlation exists between the mechanical properties and MWCNT particle size, MWCNT pre-treatment method or MWCNT density.

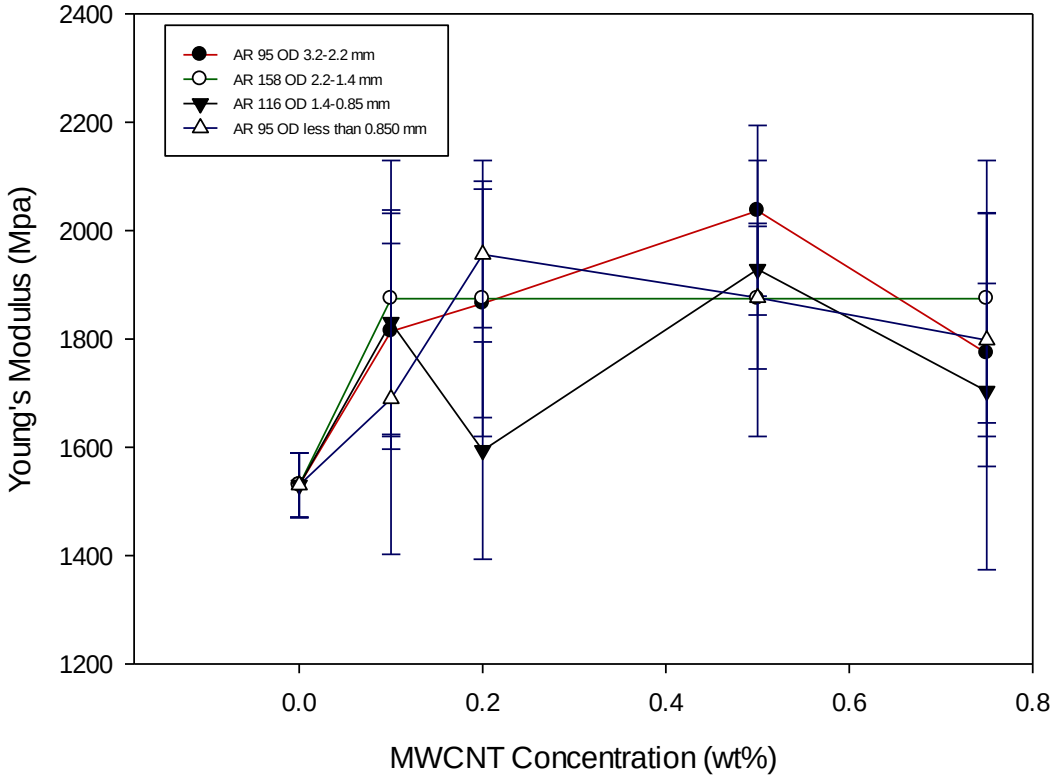

Figure 12. Young's modulus as a function of nanotube concentration for PC/MWCNT composites having different MWCNT particle sizes

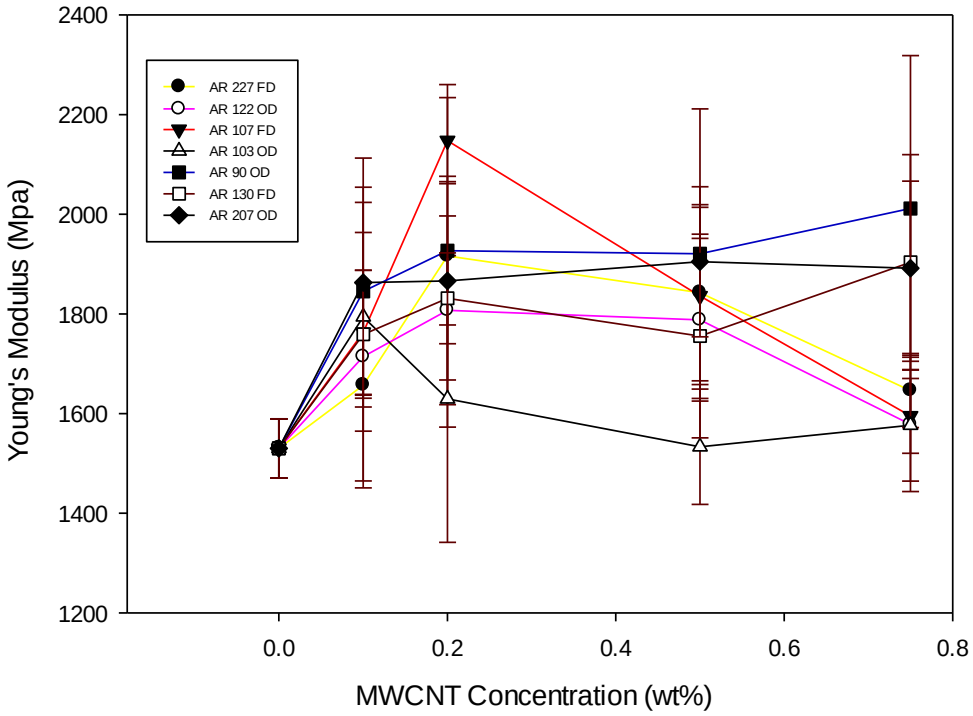

Figure 13. Young's modulus as a function of nanotube concentration for PC/MWCNT composites having different MWCNT pre-treatment methods

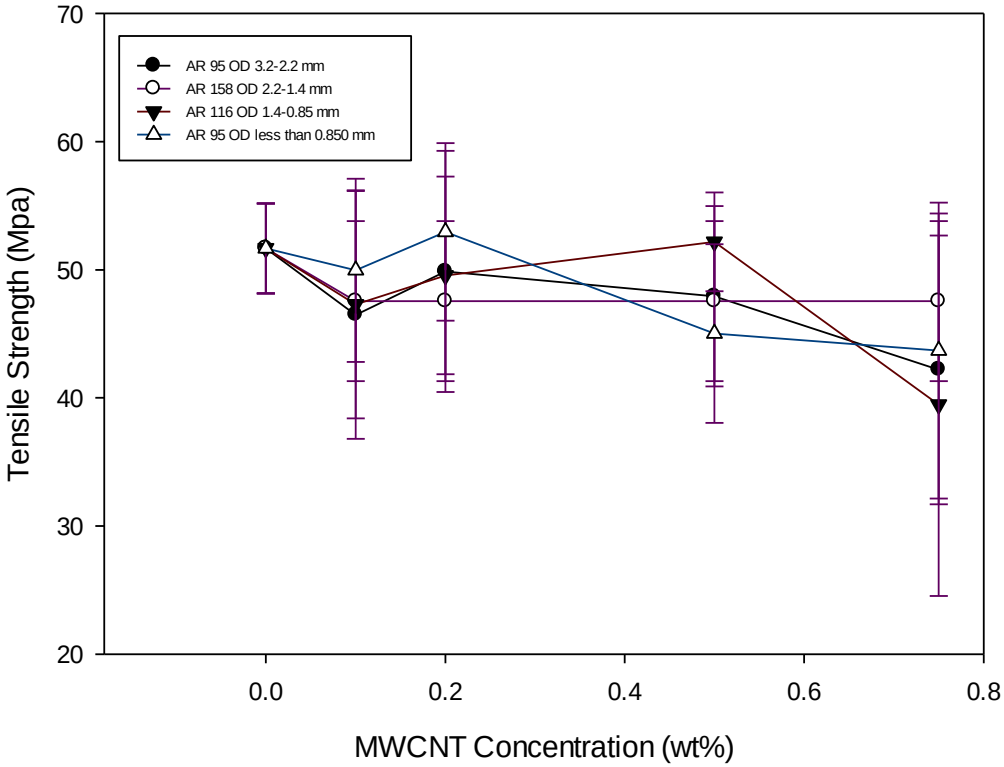

Figure 14. Tensile strength as a function of nanotube concentration for PC/MWCNT composites having different MWCNT particle sizes

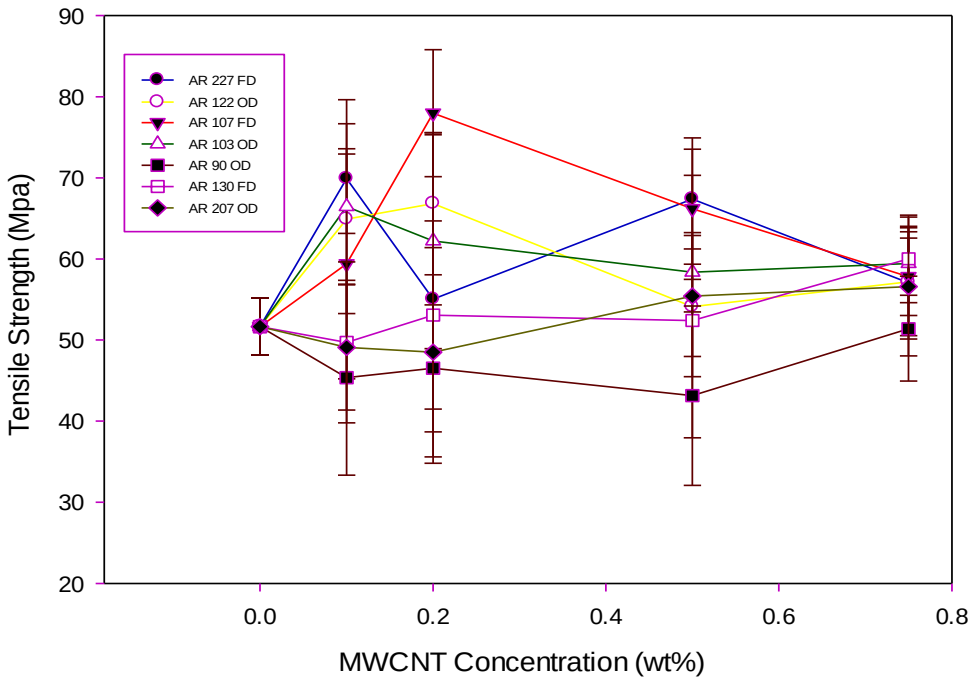

Figure 15. Tensile strength as a function of nanotube concentration for PC/MWCNT composites having different MWCNT pre-treatment methods

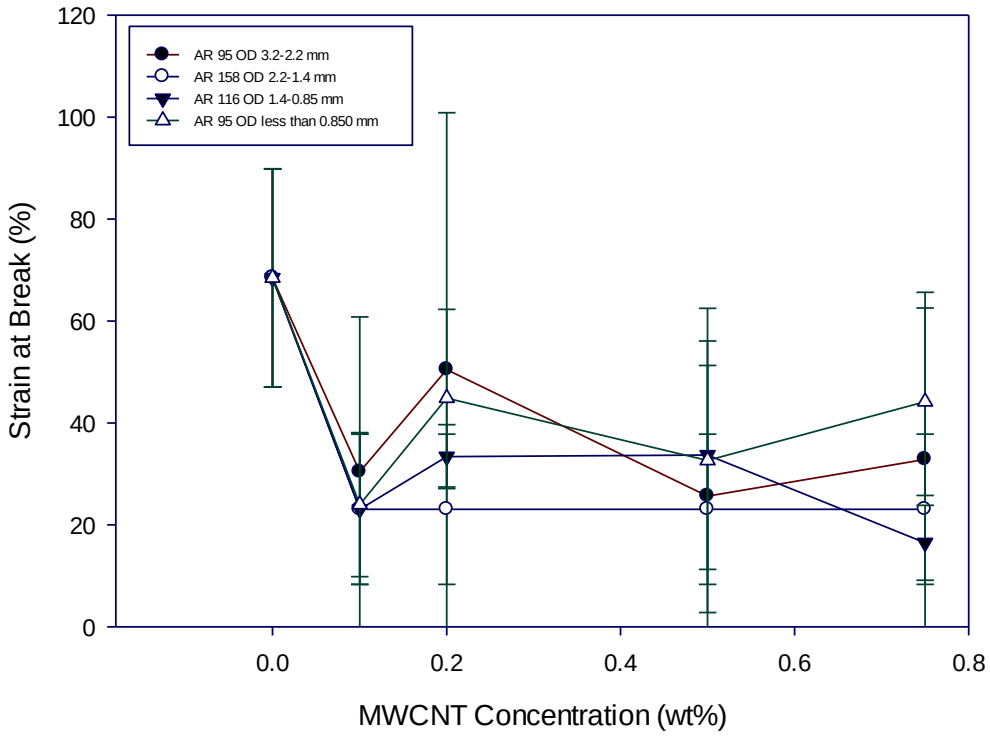

Figure 16. Strain at break as a function of nanotube concentration for PC/MWCNT composites having different MWCNT particle size

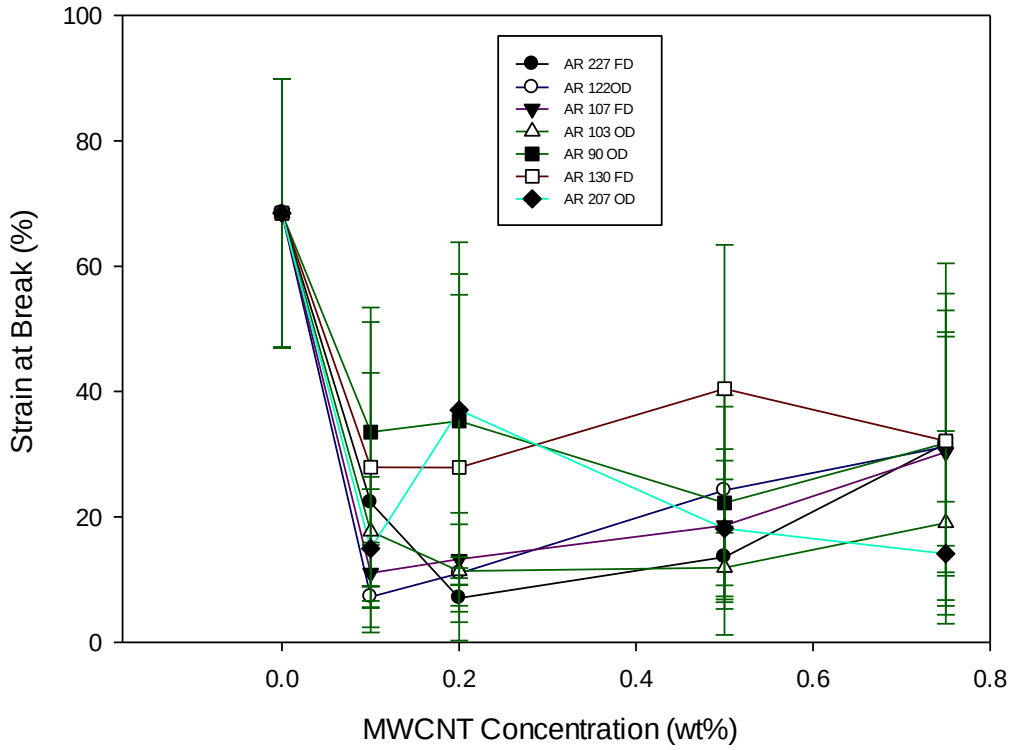

Figure 17. Strain at break as a function of nanotube concentration for PC/MWCNT composites having different MWCNT pre-treatment methods

4.5 Macro scale dispersion

4.5.1 Agglomerate area distribution

The generation of the bright field Z-stacking was chosen in this work because it eliminates the often used and time-consuming thin sectioning and at the same time provides a true agglomerate area dispersion of the entire sample. It also has the advantage of being a non-destructive method.

Figure 18 shows the statistical distribution of sizes for 0.2 wt% samples for selected composites. The macro dispersion is very homogenous and very few agglomerates are seen. In all cases the average area ratio is less than 0.18% and the average agglomerate

area is equal or less than 63.10 μm^2. Hence, agglomeration at macroscale is probably not the dominant factor in determining the percolation threshold. Additionally, the aspect ratio shape factor (the circularity) was quantified to evaluate how close the aggregates are to a circular shape. A shape factor near zero is typical of very elongated particles while close to 1 is for circular particles.

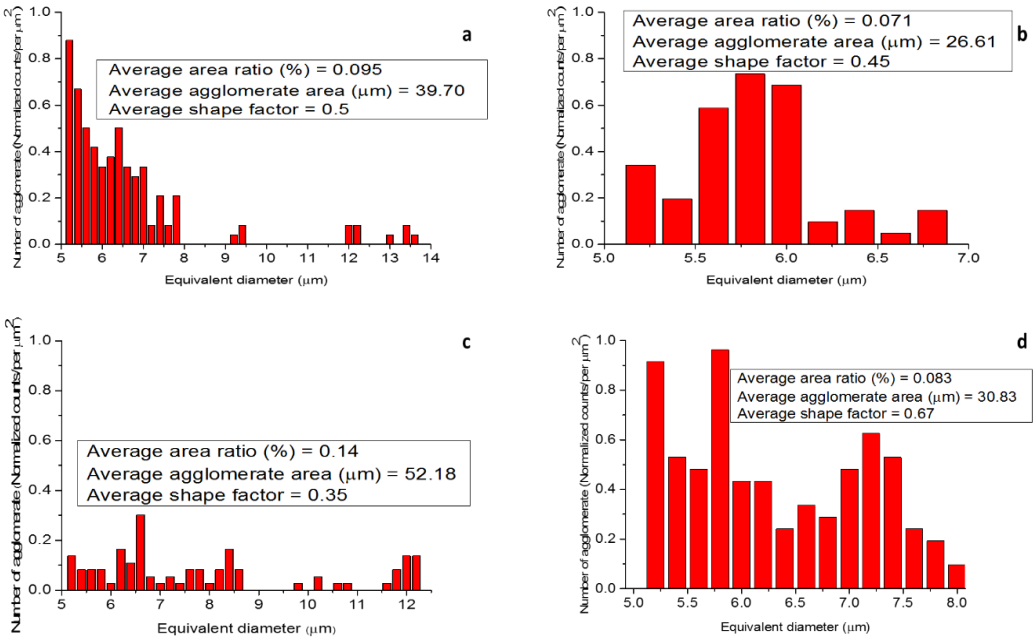

Figure 18. Agglomerate area distribution based on optical section of selected nanocomposites at 0.2 wt%: a) AR 227 FD b) AR 122 OD c) AR 158 OD <30, 2.2-1.4 mm d) AR 94 UNP

Table 7, quantifies the results from optical microscopy. All the FD MWCNTs presented a higher average agglomerate area and average area ratio than the OD MWCNTs. As was seen section 4.1.1, this difference is not enough to affect the percolation threshold of the composites. Both the average area ratio and the average

agglomerate area increase when the powder size increases. The carbon nanotube length does not seem to affect macro scale dispersion.

Table 7. Area ratio, average agglomerate area and shape factor for all composites obtained from optical sections

Sample	Average area ratio (%)	Average agglomerate area (μm^2)	Average shape factor - Circularity
AR 107 FD	0.110	40.33	0.42
AR 130 FD	0.167	62.22	0.39
AR 227 FD	0.095	39.70	0.50
AR 90 OD	0.090	35.30	0.57
AR 103 OD	0.070	25.44	0.49
AR 122 OD	0.071	26.61	0.45
AR 207 OD	0.092	36.46	0.51
AR 95 OD <30, 3.2-2.2 mm	0.170	63.10	0.47
AR 158 OD <30, 2.2-1.4 mm	0.140	52.18	0.35
AR 116 OD <30, 1.4-0.85 mm	0.108	40.45	0.54
AR 95 OD <30, < 0.850 mm	0.098	36.38	0.43
AR 82 UNP	0.093	34.74	0.57
AR 94 UNP	0.083	30.83	0.67
AR 107 UNP	0.090	33.40	0.70

4.5.2 Volume distribution

Figure 19 presents an example of the generated volume from the transmitted bright field slices taken at different angles. The agglomerates appear to be distorted in the z-direction, i.e. the thickness direction while the other two dimensions remain intact.

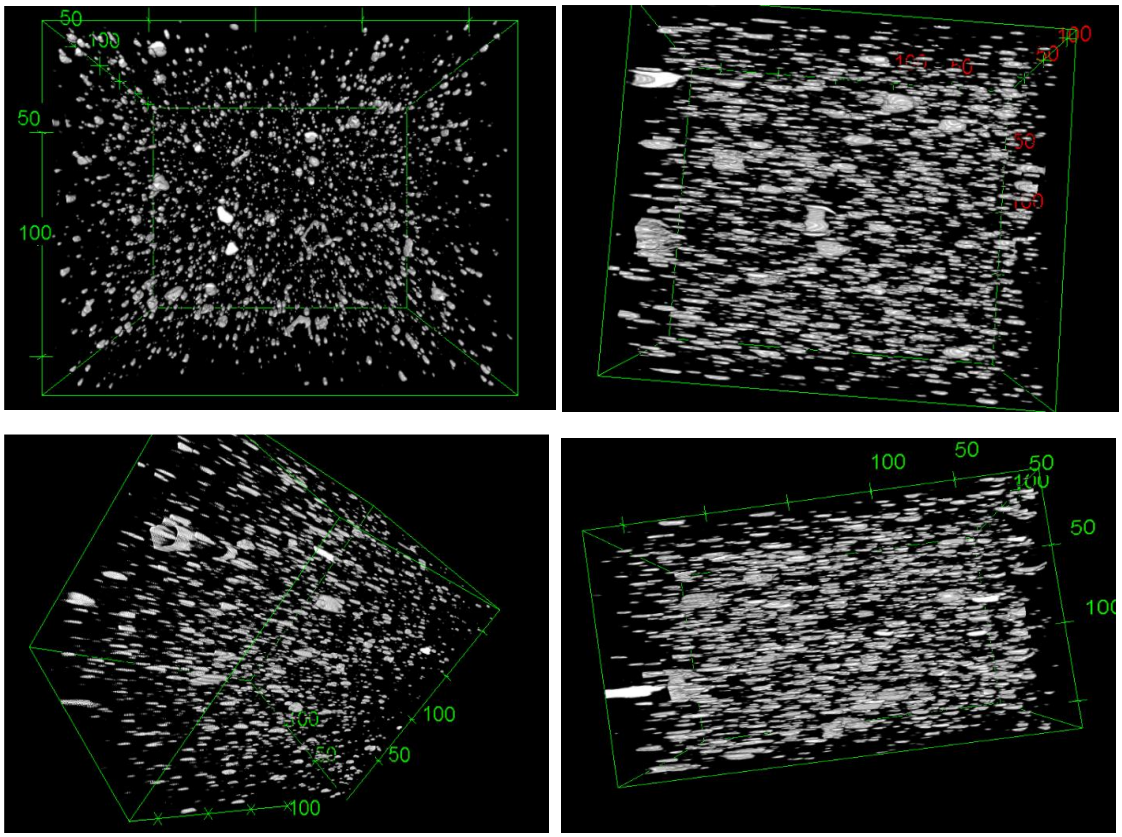

Figure 19. Generated volume distribution at different angles.

Calculating the volume of particles by averaging the lateral dimensions (X and Y), normalizes all elliptical agglomerates to spheres. This approach is commonly used to find the volume of tumors when the depth of the tumor is unknown [103]. Obviously, with this approach, the size of individual agglomerates are not determined exactly but the distribution of many of those agglomerates can de statistically described.

This methodology is different from stereological methods that have been developed to generate the volume distribution of carbon nanotubes agglomerates from thin sliced sections [104, 105] because slicing can cut through aggregates, so that the imaged aggregate could be only a piece of a larger aggregate. In this case, the methodology used in this work to generate the volume distributions has several

advantages over the traditional thin sectioning. It would be very difficult and time-consuming to obtain cross-sections of a whole sample in thin sectioning in order obtain the volume distributions while the methodology used in this work, require only a couple of minutes to generate the volume distribution. Another advantage comes from the fact that the dimensions of the agglomerates seen in a thin section micrograph are not necessarily the true dimensions and hence micrographs obtained with thin sectioning are not suitable for estimating volume distributions.

Figure 20, shows histograms of the agglomerate volume distribution for three selected composites that can be described by a log-normal distribution. The corresponding probability plot confirmed that the agglomerate were log-normally distributed. All other samples presented the same pattern.

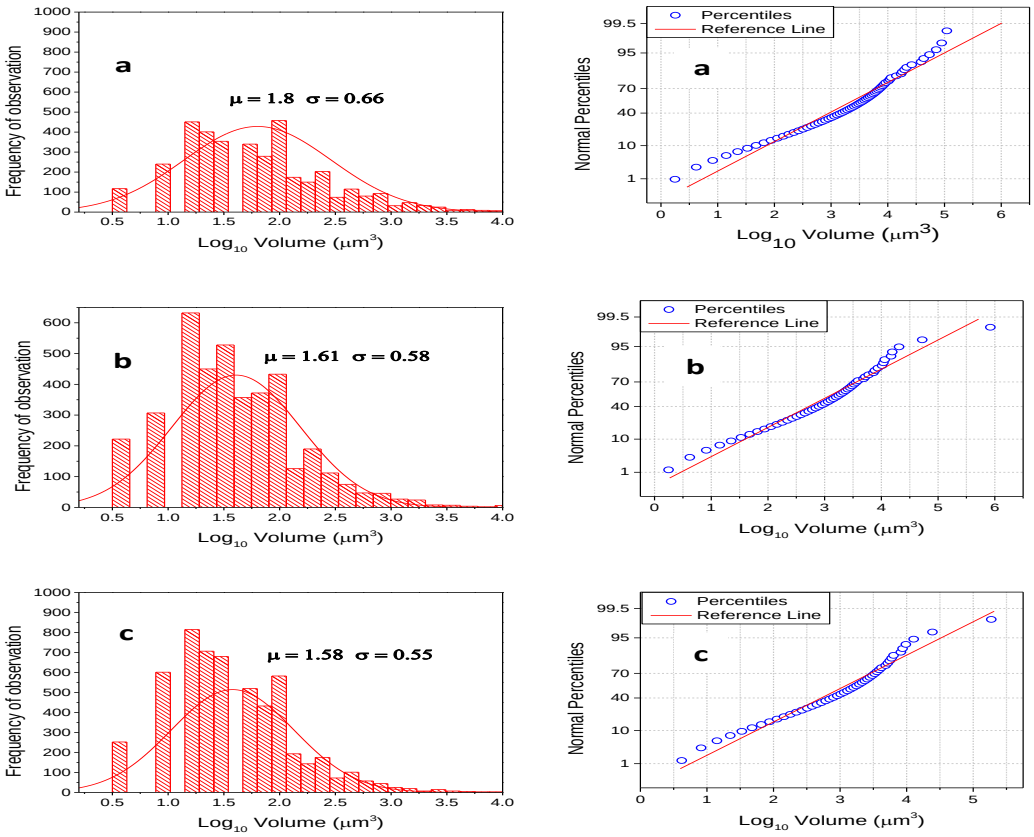

Figure 20. Left: Histogram of agglomerate volume distribution with curve showing the corresponding log-normal distribution. Right: Corresponding probability plot showing he agglomerate volume distribution relative to a log-normal distribution. a) AR 207 OD b) AR 227 FD and c) AR 158 OD >30, 2.2-1.4 mm

All samples deviate from the log-normal distribution in the lower tail at about 1.7 μm^3 (50 μm^3 in no logarithmic scale) and in the upper tail at about 4 μm^3 (10000 μm^3 in no logarithmic scale).The null hypothesis that the agglomerates volumes had a log normal distribution was accepted at 0.05 level of confidence by Shapiro-Wilk, Lilliefors, Kolgomorov-Smirnov, Anderson-Darling, D'Agostino-K squared and Chen-Shapiro normality test methods, proving that the deviation from both tails are not significant.

Since a log-normal distribution can be completely characterized by the mean and standard deviation of the log of the volume, Table 8 shows the mean and standard deviation of all composites prepared in this study.

Table 8. Mean and standard deviation for volume log-normal distribution of all composites

Samples	Mean Log volume (μm^3)	Standard deviation (μm^3)
AR 107 FD	1.65	0.61
AR 130 FD	1.64	0.60
AR 227 FD	1.61	0.58
AR 90 OD	1.54	0.53
AR 103 OD	1.63	0.60
AR 122 OD	1.80	0.66
AR 207 OD	1.55	0.56
AR 95 OD <30, 3.2-2.2 mm	1.59	0.60
AR 158 OD <30, 2.2-1.4 mm	1.58	0.55
AR 116 OD <30, 1.4-0.85 mm	1.61	0.57
AR 95 OD <30, < 0.850 mm	1.60	0.60
AR 82 UNP	1.70	0.61
AR 94 UNP	1.69	0.58
AR 107 UNP	1.67	0.56

4.6 Micro state dispersion

Figure 21 presents SEM micrographs of the primary agglomerate structure of a selected as received oven (AR 122 OD) and freeze dried (AR 227 FD) MWCNT. All oven dried and freeze dried samples presented similar agglomerate structures.

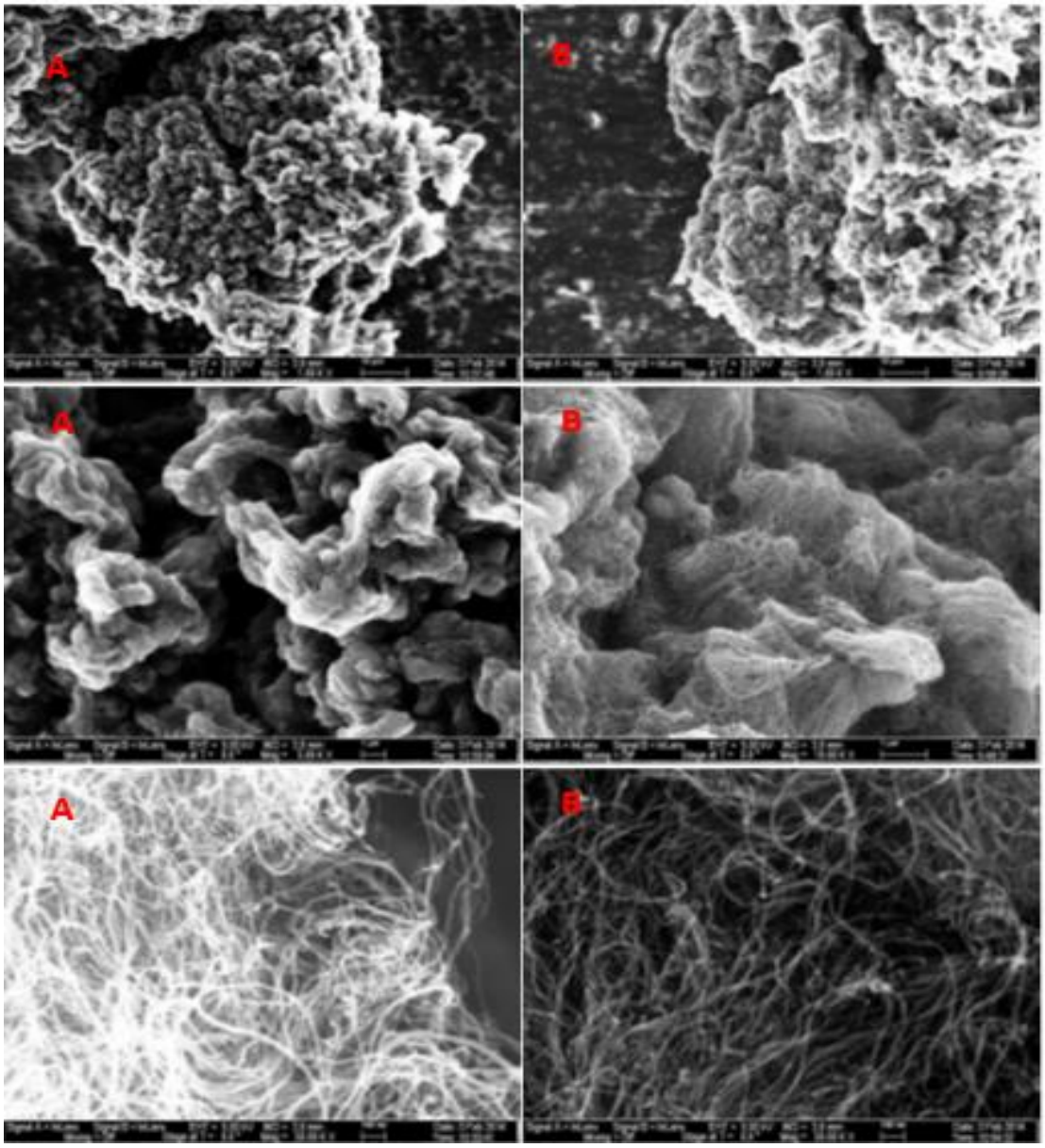

Figure 21. Scanning electron microscopy images of oven dried (AR 122 OD) (A) and freeze dried (AR 227 FD) (B) MWCNTs at three different magnifications. The upper pictures are 10 µm, the middle pictures are 1 µm and the lower pictures are 100 nm.

It can be seen qualitatively from Figure 21 that the FD sample has a more relative loose packed agglomerate structure whereas the OD sample has a more compact structure in agreement with the low and high density of the FD and OD samples, respectively. Both

OD and FD samples present a characteristic “combed yarn” structure that is more evident for the FD sample.

The dispersion at a sub-micron scale of MWCNTs, with different powder sizes and pre-treatment methods, in the PC matrix is illustrated in Figure 22 and Figure 23, respectively for composites containing 1 wt% MWCNT content. Both figures show that at the sub-micron scale, all FD and OD samples along with MWCNTs with different powder sizes exhibit a comparable dispersion.

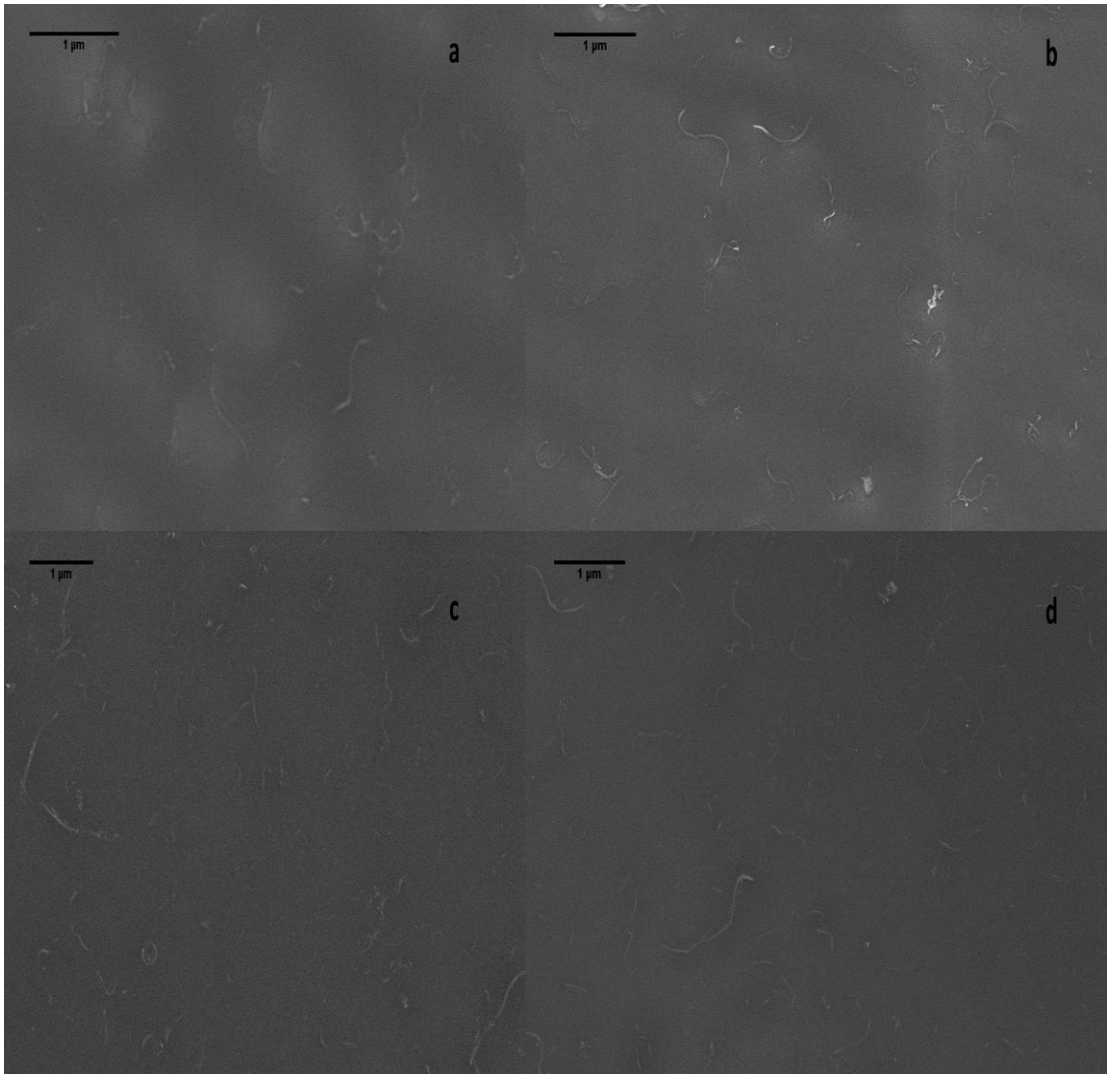

Figure 22. SEM micrographs of composites with a) AR 95 OD <30, < 0.850 mm b) AR 116 OD <30, 1.4-0.85 mm c) AR 158 OD <30, 2.2-1.4 mm d) AR 95 OD <30, 3.2-2.2 mm at 1 wt%.

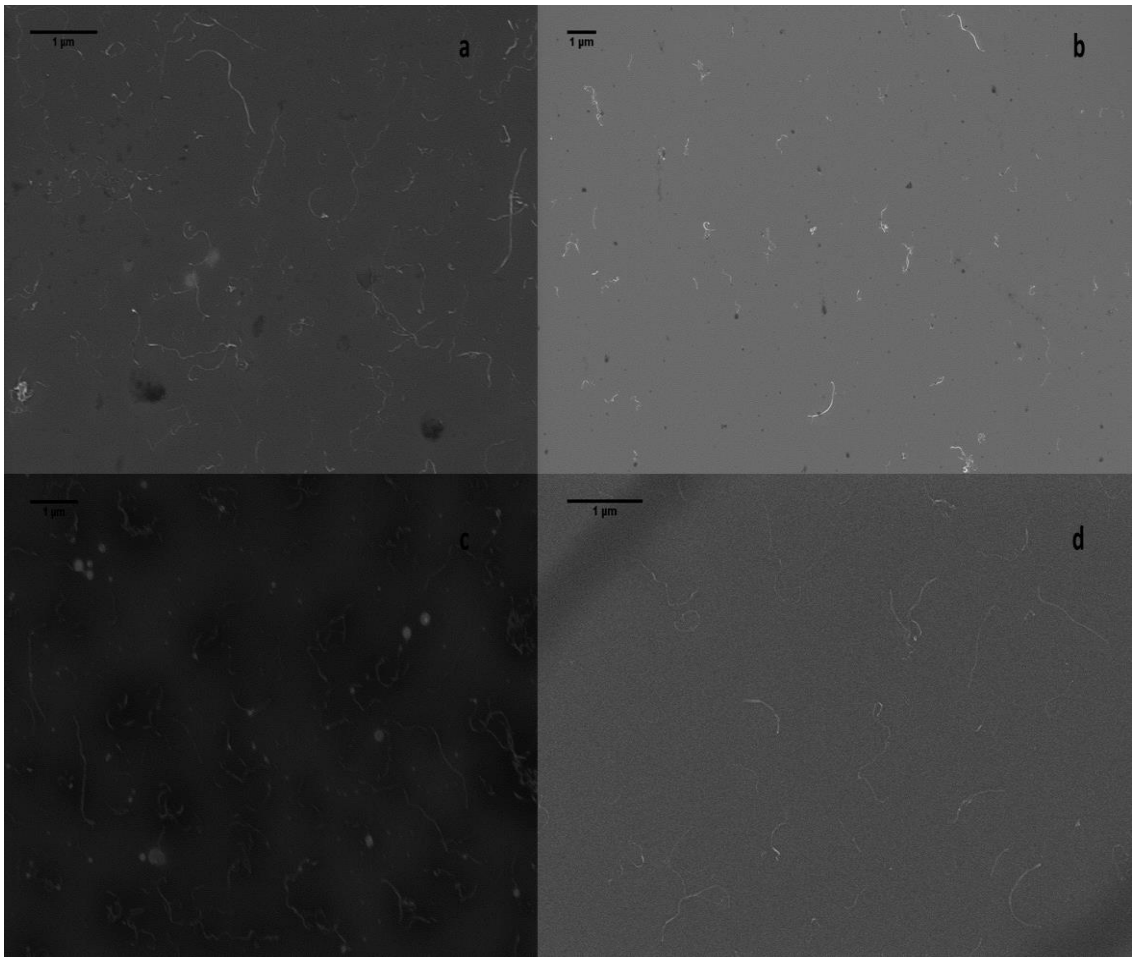

Figure 23. SEM micrographs of selected composites prepared with a) AR 122 OD b) AR 227 FD c) AR 103 OD d) AR 130 FD at 1 wt%.

Figure 24 presents SEM micrographs of composites prepared with as-received FD and OD MWCNTs submitted to an additional drying. Composites prepared with AR 227 FD and AR 103 OD with an additional drying (Figure 24c and Figure 24d), presented a similar dispersion as the ones shown in Figure 23 for composites prepared with oven dried and freeze dried nanotubes without an additional drying. Interestingly, composites prepared with AR 107 FD and AR 122 OD (Figure 24a and Figure 24b) have a considerably less carbon nanotube density than the other two composites with the additional drying, which correlates to the higher percolation thresholds exhibited by these

samples when compare with composites prepared with AR 227 FD and AR 103 OD. Although a higher percolation threshold would suggest a higher area ratio, the macro state dispersions of these samples, as measured by the area ratio, are almost identical (See section 4.5.1). This and the fact that percolation threshold does not depend on aspect ratio (L/D), implies that the dispersion at sub-micron scale is the most dominant factor to modify the electrical properties when nanotubes are submitted to an additional drying.

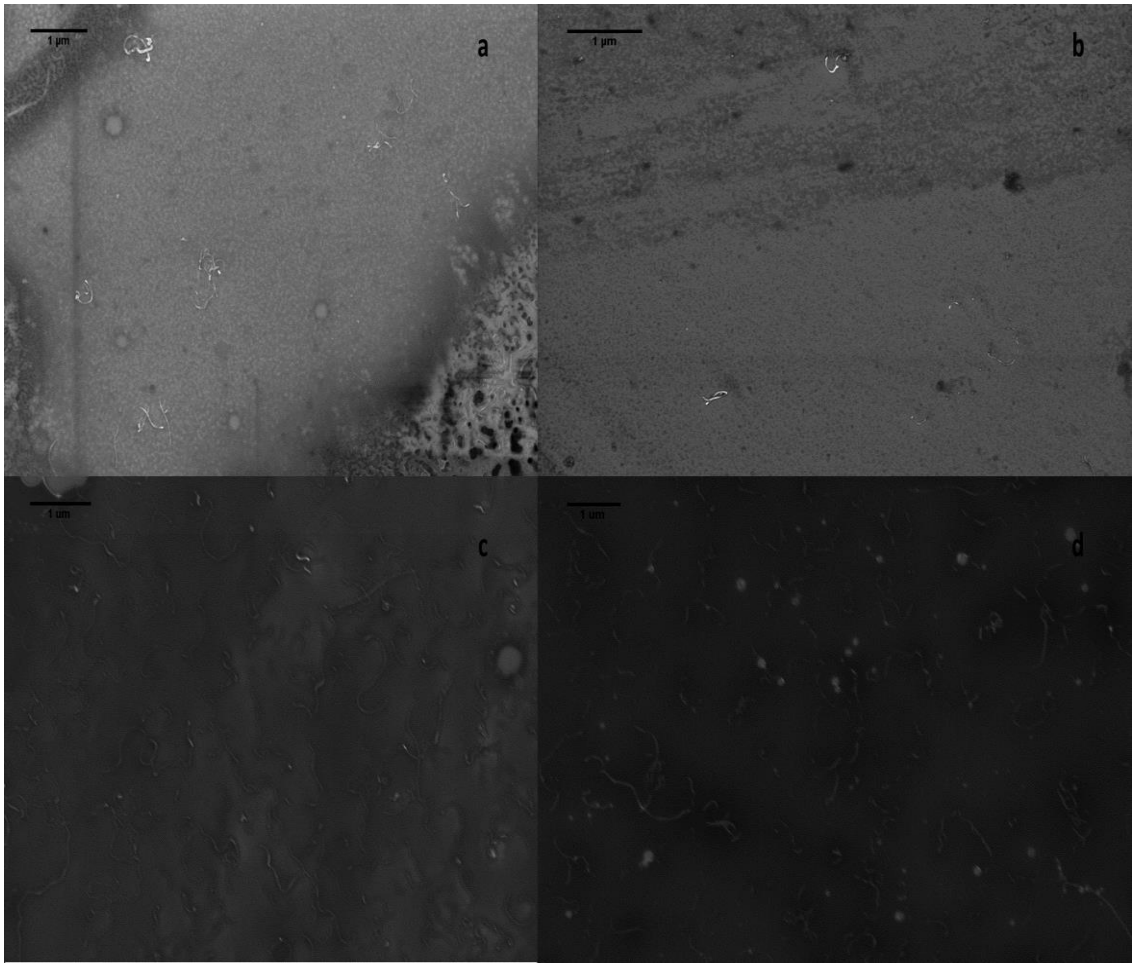

Figure 24. SEM micrographs of selected composites having an additional drying with a) AR 107 FD b) AR 122 OD c) AR 227 FD d) AR 103 OD at 1 wt%.

4.7 Thermal Analysis

Figure 25, shows thermogravimetric thermograms collected at 3 K/min for four MWCNTs: two oven-dried, one freeze-dried and one unpurified. First, all the dried tubes have a residual mass of less than 5% (They are more than 95% pure) while the unpurified MWCNT have a residual mass of about 16%. The remaining mass in the AR 94-UNP MWCNT is likely catalyst support and residual metal catalyst. Second, the two oven-dried nanotubes exhibit almost identical curves, which proves that the thermal properties of these samples do not depend on the CNT length. The freeze-dried sample is shifted to the left (i.e. degradation occurs at lower temperature), compared with the oven-dried samples.

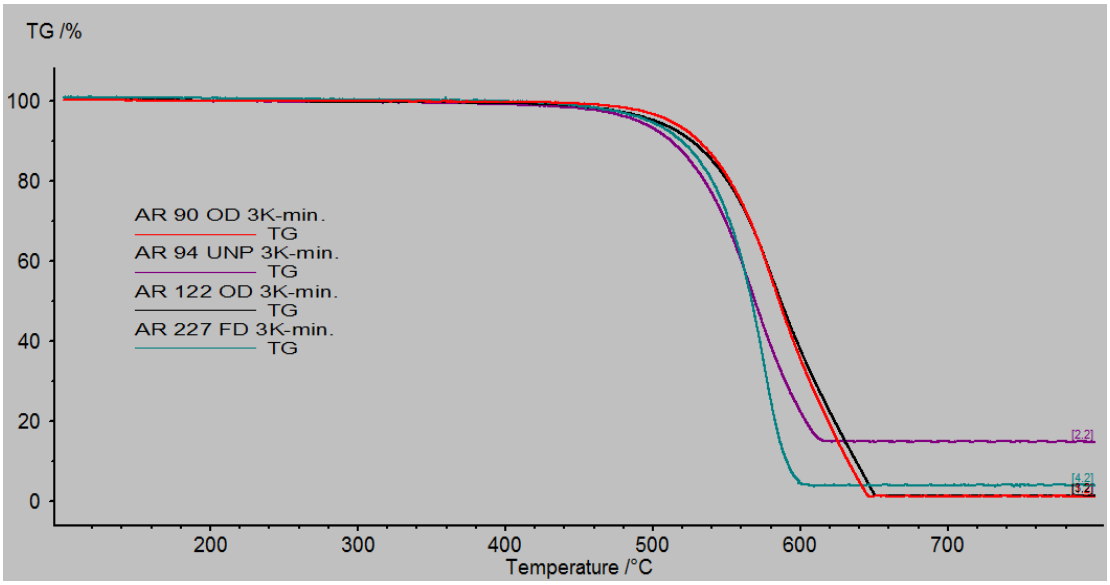

Figure 25. Thermograms of four selected samples that were oven, freeze dried and unpurified at 3 K/min.

Figure 26, shows thermograms of an oven and a freeze dried sample at a rate of 1 K/min. It can be seen that when the heating rate decreases, the curves almost merge. This result is an example of a mass transfer limitation effect, showing that the tubes are not

chemical different and providing a qualitatively way to assess the dispersion of the freeze and oven dried samples. Our belief is that this result is general. If the dispersion of the CNTs is very compacted then degradation will occur at higher temperature (i.e. the thermogram curve will shift to the right) when compared with the case where the CNTs have a less compact dispersion and the distance between the curves will become larger as the heating rate increases and shorter as the heating rate decreases. To further justify this statement, Figure 27 shows the thermograms at 3 K/min of an as-received freeze dried sample and a freeze dried sample that was compressed in a press for several minutes. The freeze dried sample curve shifts to the right just by compressing it (i.e. increasing the density). Hence, we believe that TGA can be used as a surrogate measure for density for carbon nanotubes.

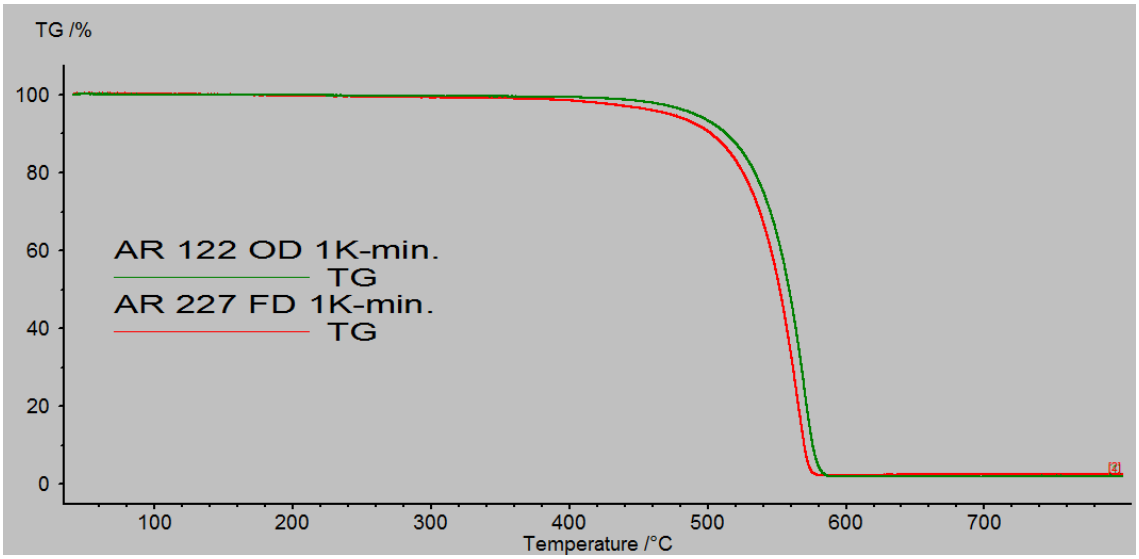

Figure 26. Thermograms of two selected oven and freeze dried MWCNTs at 1 K/min.

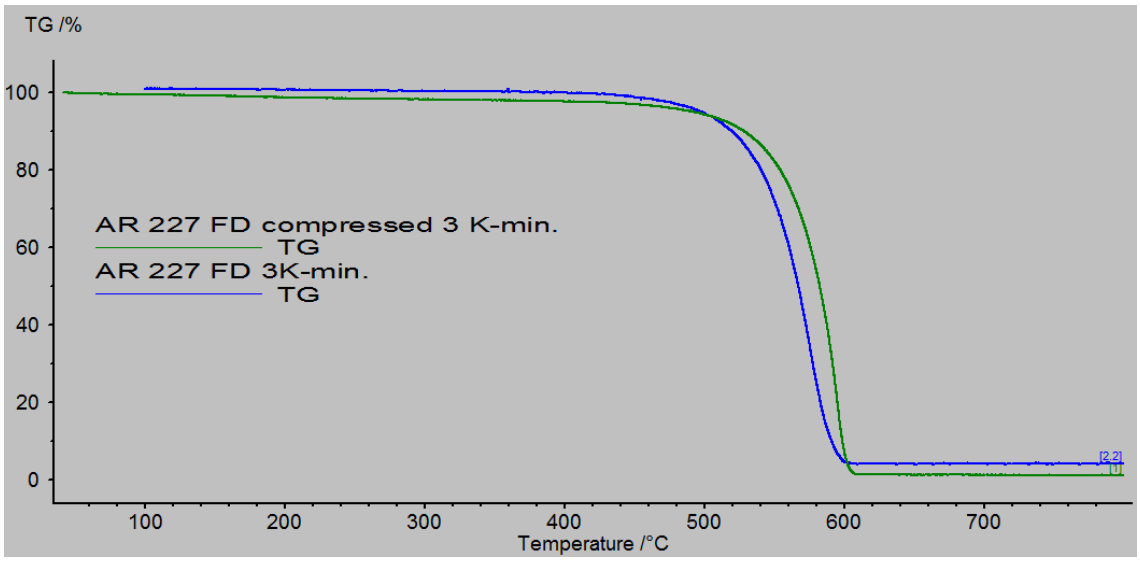

Figure 27. Thermograms of a selected freeze dried MWCNT at 3 K/min that in the as received state and compressed in a press.

Chapter 5: Conclusions

Polycarbonate was mixed with MWCNTs differing in length, density, powder size and pre-treatment method. The electrical and mechanical properties were studied and correlated with the state of dispersion of the MWCNTs. It was shown that processing in the conical twin-screw under the conditions used in this work, reduces the length of the MWCNTs with higher starting lengths more than the MWCNTs with lower starting lengths and that the carbon nanotube characteristics under study showed to have no effect on the breakage of the tubes during processing.

The addition of nanotubes with different lengths, densities, powder sizes and pre-treatment methods did not have any effect on the mechanical properties. The Young's modulus and tensile strength slightly increases while the strain at break drastically decreases only when compare with polycarbonate with no nanotube content.

The classical percolation theory predicts a dependence of the percolation threshold with the inverse of the aspect ratio and does not take into account other key factors to predict the percolation threshold. The values of the percolation threshold can be seen as a function of both carbon nanotube dispersion and geometry (i.e. aspect ratio, shape, waviness). Light microscopy and SEM provided insight into the state of dispersion of MWCNTs with different characteristics at different scales. At submicron scale, the state of dispersion of all MWCNTs were comparable independently of length, pre-treatment method, density or powder size. At macro scale, both agglomerate area and area ratio were shown to increase as powder size increases and to be larger for freeze-dried

MWCNTs than for oven-dried MWCNTs. However, the differences in the agglomerate area and area ratio were not appreciable enough to modify the percolation threshold of their composites when compare with pre-treated nanotubes with other characteristics. The waviness of the MWCNTs and the fact that their lengths (or aspect ratios) did not affect the dispersion at any of the scales analyzed, was suggested to be the main caused for contradictory theoretical expectations based on classical percolation theory. In this case, dispersion of the MWCNTs played a bigger role than aspect ratio on the electrical properties of PC/MWCNTs composites.

When as-received freeze-dried and oven-dried MWCNTs are submitted to an intermediate step of evaporation of water prior to melt mixing, their composites exhibit an increase in the percolation threshold only if the MWCNTs have short lengths; otherwise the percolation threshold is not affected. This was corroborated by the dispersion state at submicron scale where the shorter MWCNTs had fewer carbon nanotube dispersed than the longer MWCNTs, which may hinder their ability to form a percolated network. It was suggested that the additional drying overwrites the previous drying done to the MWCNTs and changes the state of dispersion of shorter nanotubes to one with more entanglements and agglomerates when being compacted during a drying process than longer nanotubes due to pre-existing entanglements for the latter case. Further, since key literature introduce an additional drying method to the nanotubes and additionally acid treat them, it was suggested that the decrease in electrical properties and dispersion for oven-dried MWCNTs when compared with freeze-dried MWCNTs reported in the literature, is an effect of both shorter tubes generated during the first drying

process, and on the compaction of the generated short tubes during a second drying to remove any water gained.

The drying method improved the dispersability of the MWCNTs when compare with unpurified samples based on a simple test involving dispersion in chloroform. It was shown by SEM and TGA that the initial freeze-dried MWCNTs had a more loose packed agglomerate structure than the oven-dried MWCNTs, consistent with density measurements. The structure of the agglomerate, however, did not affect the percolation thresholds exhibited by all composites.

Finally, TGA and bright field light microscopy proved to be useful techniques to evaluate carbon nanotube characteristics. TGA was shown to be useful as a surrogate method to evaluate CNT density and dispersion. On the other hand, the generation of a bright field Z-stacking with light microscopy, besides being non-destructive and eliminating the need for the time-consuming thin sectioning, can be used to describe the volume distribution of carbon nanotubes agglomerates. The volume distribution were described by a log-normal distribution for all samples.

References

1. Iijima, S., *Helical Microtubules of Graphitic Carbon.* Nature, 1991. **354**(6348): p. 56-58.

2. Chen, S.J., et al., *Predicting the influence of ultrasonication energy on the reinforcing efficiency of carbon nanotubes.* Carbon, 2014. **77**: p. 1-10.

3. Zhou, Y.X., et al., *Improvement in electrical, thermal and mechanical properties of epoxy by filling carbon nanotube.* Express Polymer Letters, 2008. **2**(1): p. 40-48.

4. Hollertz, R., et al., *Improvement of toughness and electrical properties of epoxy composites with carbon nanotubes prepared by industrially relevant processes.* Nanotechnology, 2011. **22**(12).

5. Alig, I., et al., *Establishment, morphology and properties of carbon nanotube networks in polymer melts.* Polymer, 2012. **53**(1): p. 4-28.

6. Andrews, R., et al., *Fabrication of carbon multiwall nanotube/polymer composites by shear mixing.* Macromolecular Materials and Engineering, 2002. **287**(6): p. 395-403.

7. Jin, Z., et al., *Dynamic mechanical behavior of melt-processed multi-walled carbon nanotube/poly(methyl methacrylate) composites.* Chemical Physics Letters, 2001. **337**(1-3): p. 43-47.

8. Sandler, J., et al., *Development of a dispersion process for carbon nanotubes in an epoxy matrix and the resulting electrical properties.* Polymer, 1999. **40**(21): p. 5967-5971.

9. Cooper, C.A., et al., *Distribution and alignment of carbon nanotubes and nanofibrils in a polymer matrix.* Composites Science and Technology, 2002. **62**(7-8): p. 1105-1112.

10. Guo, J.X., et al., *Aspect Ratio Effects of Multi-walled Carbon Nanotubes on Electrical, Mechanical, and Thermal Properties of Polycarbonate/MWCNT Composites.* Journal of Polymer Science Part B-Polymer Physics, 2014. **52**(1): p. 73-83.

11. Pötschke, P., S.M. Dudkin, and I. Alig, *Dielectric spectroscopy on melt processed polycarbonate—multiwalled carbon nanotube composites.* Polymer, 2003. **44**(17): p. 5023-5030.

12. Bose, S., R.A. Khare, and P. Moldenaers, *Assessing the strengths and weaknesses of various types of pre-treatments of carbon nanotubes on the properties of polymer/carbon nanotubes composites: A critical review.* Polymer, 2010. **51**(5): p. 975-993.

13. Moniruzzaman, M. and K.I. Winey, *Polymer nanocomposites containing carbon nanotubes.* Macromolecules, 2006. **39**(16): p. 5194-5205.

14. Lu, K.L., et al., *Mechanical damage of carbon nanotubes by ultrasound.* Carbon, 1996. **34**(6): p. 814-816.

15. Fang, J., et al., *Freeze-drying method prepared UHMWPE/CNTs composites with optimized micromorphologies and improved tribological performance.* Journal of Applied Polymer Science, 2015. **132**(18).

16. Morcom, M., K. Atkinson, and G.P. Simon, *The effect of carbon nanotube properties on the degree of dispersion and reinforcement of high density polyethylene.* Polymer, 2010. **51**(15): p. 3540-3550.

17. Cadek, M., et al., *Reinforcement of polymers with carbon nanotubes: The role of nanotube surface area.* Nano Letters, 2004. **4**(2): p. 353-356.

18. Thostenson, E.T. and T.W. Chou, *On the elastic properties of carbon nanotube-based composites: modelling and characterization.* Journal of Physics D-Applied Physics, 2003. **36**(5): p. 573-582.

19. Sung, Y.T., et al., *Rheological and electrical properties of polycarbonate/multi-walled carbon nanotube composites.* Polymer, 2006. **47**(12): p. 4434-4439.

20. Radushkevich, L.V. and V.M. Lukyanovich, *O strukture ugleroda, obrazujucegosja pri termiceskom razlozenii okisi ugleroda na zeleznom kontakte.* Zurn Fisic Chim, 1952. **26**: p. 88-95.

21. Li, Z., *Routes towards Manufacturing Janus Carbon Nanotubes*, in *Faculty of Engineering and Physical Sciences*. 2013, University of Manchester.

22. Kroto, H.W., et al., *C-60 - Buckminsterfullerene.* Nature, 1985. **318**(6042): p. 162-163.

23. Grady, B.P., in *Carbon Nanotube–Polymer Composites: Manufacture, properties and applications*. 2011, John Wiley & Sons, Inc.

24. Mehra, N.K., V. Mishra, and N.K. Jain, *A review of ligand tethered surface engineered carbon nanotubes.* Biomaterials, 2014. **35**(4): p. 1267-1283.

25. Harris, P.J.F., *Carbon Nanotubes and Related Structures*. 1999: Cambridge University Press.

26. Shiren, W., *Functionalization of Carbon Nanotubes: Characterization, Modeling and Composite Applications*, in *Department of Industrial and Manufacturing Engineering*. 2006, Florida State University.

27. Oberlin, A., M. Endo, and T. Koyama, *Filamentous Growth of Carbon through Benzene Decomposition.* Journal of Crystal Growth, 1976. **32**(3): p. 335-349.

28. Bethune, D.S., et al., *Cobalt-Catalyzed Growth of Carbon Nanotubes with Single-Atomic-Layerwalls.* Nature, 1993. **363**(6430): p. 605-607.

29. Iijima, S. and T. Ichihashi, *Single-Shell Carbon Nanotubes of 1-Nm Diameter.* Nature, 1993. **363**(6430): p. 603-605.

30. Geim, A.K. and K.S. Novoselov, *The rise of graphene.* Nature Materials, 2007. **6**(3): p. 183-191.

31. Prasek, J., et al., *Methods for carbon nanotubes synthesis-review.* Journal of Materials Chemistry, 2011. **21**(40): p. 15872-15884.

32. Dresselhaus, M.S., G. Dresselhaus, and R. Saito, *Physics of Carbon Nanotubes.* Carbon, 1995. **33**(7): p. 883-891.

33. Dresselhaus, M.S., G. Dresselhaus, and P.C. Eklund, *Chapter 3 - Structure of Fullerenes*, in *Science of Fullerenes and Carbon Nanotubes*, M.S.D.D.C. Eklund, Editor. 1996, Academic Press: San Diego. p. 60-79.

34. Nadia, G.C., Koning., Marie-Claire, Hermant. , *Polymer Carbon Nanotube Composites: The Polymer Latex Concept* 2012: Pan Standford Publishing Pte. Ltd.

35. Terrones, M., *Science and technology of the twenty-first century: Synthesis, properties and applications of carbon nanotubes.* Annual Review of Materials Research, 2003. **33**: p. 419-501.

36. Hare, J., *Fullerene math*. 2013: http://www.geoset.info/view-presentation/?pid=9070&url=http://www.youtube.com/watch?v=Huov03jLaL0.

37. Ma, P.C., et al., *Dispersion and functionalization of carbon nanotubes for polymer-based nanocomposites: A review.* Composites Part a-Applied Science and Manufacturing, 2010. **41**(10): p. 1345-1367.

38. Wang, S.R., et al., *Statistical characterization of single-wall carbon nanotube length distribution.* Nanotechnology, 2006. **17**(3): p. 634-639.

39. Xie, X.L., Y.W. Mai, and X.P. Zhou, *Dispersion and alignment of carbon nanotubes in polymer matrix: A review.* Materials Science & Engineering R-Reports, 2005. **49**(4): p. 89-112.

40. Bandaru, P.R., *Electrical properties and applications of carbon nanotube structures.* J Nanosci Nanotechnol, 2007. **7**(4-5): p. 1239-67.

41. Bauhofer, W. and J.Z. Kovacs, *A review and analysis of electrical percolation in carbon nanotube polymer composites.* Composites Science and Technology, 2009. **69**(10): p. 1486-1498.

42. Min, C.Y., et al., *The Electrical Properties and Conducting Mechanisms of Carbon Nanotube/Polymer Nanocomposites: A Review.* Polymer-Plastics Technology and Engineering, 2010. **49**(12): p. 1172-1181.

43. Barrau, S., et al., *Effect of palmitic acid on the electrical conductivity of carbon nanotubes-epoxy resin composites.* Macromolecules, 2003. **36**(26): p. 9678-9680.

44. Du, F.M., J.E. Fischer, and K.I. Winey, *Effect of nanotube alignment on percolation conductivity in carbon nanotube/polymer composites.* Physical Review B, 2005. **72**(12).

45. Haggenmueller, R., et al., *Aligned single-wall carbon nanotubes in composites by melt processing methods.* Chemical Physics Letters, 2000. **330**(3-4): p. 219-225.

46. Pegel, S., et al., *Dispersion, agglomeration, and network formation of multiwalled carbon nanotubes in polycarbonate melts.* Polymer, 2008. **49**(4): p. 974-984.

47. Yakobson, B.I. and P. Avouris, *Mechanical properties of carbon nanotubes.* Carbon Nanotubes, 2001. **80**: p. 287-327.

48. Qian, D., et al., *Mechanics of carbon nanotubes.* Applied Mechanics Reviews, 2002. **55**(6): p. 495-533.

49. Ma, P.C., B.Z. Tang, and J.K. Kim, *Effect of CNT decoration with silver nanoparticles on electrical conductivity of CNT-polymer composites.* Carbon, 2008. **46**(11): p. 1497-1505.

50. Kosmidou, T.V., et al., *Structural, mechanical and electrical characterization of epoxy-amine/carbon black nanocomposites.* Express Polymer Letters, 2008. **2**(5): p. 364-372.

51. Tyson, B.M., et al., *A quantitative method for analyzing the dispersion and agglomeration of nano-particles in composite materials.* Composites Part B-Engineering, 2011. **42**(6): p. 1395-1403.

52. Bing, D., *Functionalization of Multi-walled Carbon Nanotubes and Localization of Functionalized Multi-walled Carbon Nanotubes in an SAN/PPE Blend*, in *Department of Chemistry*. 2013, Universität Hamburg.

53. de Luna, M.S., et al., *Importance of the morphology and structure of the primary aggregates for the dispersibility of carbon nanotubes in polymer melts.* Composites Science and Technology, 2013. **85**: p. 17-22.

54. Song, Y.S. and J.R. Youn, *Influence of dispersion states of carbon nanotubes on physical properties of epoxy nanocomposites.* Carbon, 2005. **43**(7): p. 1378-1385.

55. Fu, X., et al., *Quantitative evaluation of carbon nanotube dispersion through scanning electron microscopy images.* Composites Science and Technology, 2013. **87**: p. 170-173.

56. Dong, L.B., et al., *Comparison of drying methods for the preparation of carbon fiber felt/carbon nanotubes modified epoxy composites.* Composites Part a-Applied Science and Manufacturing, 2013. **55**: p. 74-82.

57. Park, W.K., et al., *Effect of carbon nanotube pre-treatment on dispersion and electrical properties of melt mixed multi-walled carbon nanotubes/poly(methyl methacrylate) composites.* Macromolecular Research, 2005. **13**(3): p. 206-211.

58. Dong, L.B., et al., *Spatial dispersion state of carbon nanotubes in a freeze-drying method prepared carbon fiber based preform and its effect on electrical conductivity of carbon fiber/epoxy composite.* Materials Letters, 2014. **130**: p. 292-295.

59. Dong, L.B., et al., *Combination effect of physical drying with chemical characteristic of carbon nanotubes on through-thickness properties of carbon fiber/epoxy composites.* Journal of Materials Science, 2014. **49**(14): p. 4979-4988.

60. Maugey, M., et al., *Substantial improvement of nanotube processability by freeze-drying.* Journal of Nanoscience and Nanotechnology, 2007. **7**(8): p. 2633-2639.

61. Dong, L.B., et al., *Preparation of continuous carbon nanotube networks in carbon fiber/epoxy composite.* Composites Part a-Applied Science and Manufacturing, 2014. **56**: p. 248-255.

62. Rinzler, J.W.A.a.A.G. *Deposition of Optical Thin Films of Nanotubes* [cited 2015 August 2].

63. Bryning, M.B., et al., *Carbon nanotube aerogels.* Advanced Materials, 2007. **19**(5): p. 661-+.

64. Nakagawa, K., et al., *Freeze-dried solid foams prepared from carbon nanotube aqueous suspension: Application to gas diffusion layers of a proton exchange membrane fuel cell.* Chemical Engineering and Processing, 2011. **50**(1): p. 22-30.

65. Thongprachan, N., et al., *Preparation of macroporous solid foam from multi-walled carbon nanotubes by freeze-drying technique.* Materials Chemistry and Physics, 2008. **112**(1): p. 262-269.

66. Sun, H.Y., Z. Xu, and C. Gao, *Multifunctional, Ultra-Flyweight, Synergistically Assembled Carbon Aerogels.* Advanced Materials, 2013. **25**(18): p. 2554-2560.

67. Wang, L., et al., *Preparation and Mechanical Properties of Continuous Carbon Nanotube Networks Modified Cf/SiC Composite.* Advances in Materials Science and Engineering.

68. Hirsch, A. and C. Backes, *Carbon Nanotube Science. Synthesis, Properties and Applications. By Peter J. F. Harris.* Angewandte Chemie International Edition, 2010. **49**(10): p. 1722-1723.

69. Huang, Y., et al., *The influence of single-walled carbon nanotube structure on the electromagnetic interference shielding efficiency of its epoxy composites.* Carbon, 2007. **45**(8): p. 1614-1621.

70. Simien, D., et al., *Influence of nanotube length on the optical and conductivity properties of thin single-wall carbon nanotube networks.* Acs Nano, 2008. **2**(9): p. 1879-1884.

71. Kasaliwal, G.R., et al., *4 - Influence of material and processing parameters on carbon nanotube dispersion in polymer melts*, in *Polymer–Carbon Nanotube Composites*, T. McNally and P. Pötschke, Editors. 2011, Woodhead Publishing. p. 92-132.

72. Martins, J.N., et al., *Poly(vinylidene fluoride)/polyaniline/carbon nanotubes nanocomposites: Influence of preparation method and oscillatory shear on morphology and electrical conductivity.* Polymer Testing, 2013. **32**(8): p. 1511-1521.

73. Galano, A., *On the influence of diameter and length on the properties of armchair single-walled carbon nanotubes: A theoretical chemistry approach.* Chemical Physics, 2006. **327**(1): p. 159-170.

74. Spitalsky, Z., et al., *Carbon nanotube-polymer composites: Chemistry, processing, mechanical and electrical properties.* Progress in Polymer Science, 2010. **35**(3): p. 357-401.

75. Krause, B., et al., *Comparison of nanotubes produced by fixed bed and aerosol-CVD methods and their electrical percolation behaviour in melt mixed polyamide 6.6 composites.* Composites Science and Technology, 2010. **70**(1): p. 151-160.

76. Krause, B., et al., *Dispersability and particle size distribution of CNTs in an aqueous surfactant dispersion as a function of ultrasonic treatment time.* Carbon, 2010. **48**(10): p. 2746-2754.

77. Socher, R., et al., *Melt mixed nano composites of PA12 with MWNTs: Influence of MWNT and matrix properties on macrodispersion and electrical properties.* Composites Science and Technology, 2011. **71**(3): p. 306-314.

78. Castillo, F.Y., et al., *Electrical, mechanical, and glass transition behavior of polycarbonate-based nanocomposites with different multi-walled carbon nanotubes.* Polymer, 2011. **52**(17): p. 3835-3845.

79. Krause, B., et al., *Influence of dry grinding in a ball mill on the length of multiwalled carbon nanotubes and their dispersion and percolation behaviour in melt mixed polycarbonate composites.* Composites Science and Technology, 2011. **71**(8): p. 1145-1153.

80. Krause, B., et al., *Correlation of carbon nanotube dispersability in aqueous surfactant solutions and polymers.* Carbon, 2009. **47**(3): p. 602-612.

81. Verge, P., et al., *Unpredictable dispersion states of MWNTs in HDPE: A comparative and comprehensive study.* European Polymer Journal, 2012. **48**(4): p. 677-683.

82. Menzer, K., et al., *Percolation behaviour of multiwalled carbon nanotubes of altered length and primary agglomerate morphology in melt mixed isotactic polypropylene-based composites.* Composites Science and Technology, 2011. **71**(16): p. 1936-1943.

83. Krause, B., R. Bolcit, and P. Potschke, *A method for determination of length distributions of multiwalled carbon nanotubes before and after melt processing.* Carbon, 2011. **49**(4): p. 1243-1247.

84. Lin, B., U. Sundararaj, and P. Potschke, *Melt mixing of polycarbonate with multi-walled carbon nanotubes in miniature mixers.* Macromolecular Materials and Engineering, 2006. **291**(3): p. 227-238.

85. Visser, T.D. and J.L. Oud, *Volume measurements in three-dimensional microscopy.* Scanning, 1994. **16**(4): p. 198-200.

86. Kolmogoroff, A.N., *The logarithmically normal law of distribution of dimensions of particles when broken into small parts.* NASA PUBLICATION, 1969.

87. Smith, B.E., H. Yazdani, and K. Hatami, *Three-dimensional imaging and quantitative analysis of dispersion and mechanical failure in filled nanocomposites.* Composites Part A: Applied Science and Manufacturing, 2015. **79**: p. 23-29.

88. Yazdani, H., B.E. Smith, and K. Hatami, *Multi-walled carbon nanotube-filled polyvinyl chloride composites: Influence of processing method on dispersion quality, electrical conductivity and mechanical properties.* Composites Part A: Applied Science and Manufacturing, 2016. **82**: p. 65-77.

89. Institution, B.S., *BS ISO 18553:2002*. 2002: BSI.

90. J. Guo, Y.L., R. Prada-Silvy, Y. Tan, S. Azad, B. Krause, P. Pötschke, B.P. Grady, 2014. **52**.

91. Liu, C.-X. and J.-W. Choi, *Improved Dispersion of Carbon Nanotubes in Polymers at High Concentrations.* Nanomaterials, 2012. **2**(4): p. 329.

92. Yu, Y., et al., *Influence of filler waviness and aspect ratio on the percolation threshold of carbon nanomaterials reinforced polymer nanocomposites.* Journal of Materials Science, 2013. **48**(17): p. 5727-5732.

93. Lee, H.S., et al., *Percolation of two-dimensional multiwall carbon nanotube networks.* Applied Physics Letters, 2009. **95**(13): p. 134104.

94. Cao, G., et al., *Infiltration behaviour of water in a carbon nanotube under external pressure.* Philosophical Magazine Letters, 2008. **88**(5): p. 371-378.

95. Rossi, M.P., et al., *Environmental Scanning Electron Microscopy Study of Water in Carbon Nanopipes.* Nano Letters, 2004. **4**(5): p. 989-993.

96. Dujardin, E., et al., *Wetting of Single Shell Carbon Nanotubes.* Advanced Materials, 1998. **10**(17): p. 1472-1475.

97. Dujardin, E., et al., *Capillarity and Wetting of Carbon Nanotubes.* Science, 1994. **265**(5180): p. 1850-1852.

98. Aria, A.I. and M. Gharib, *Dry Oxidation and Vacuum Annealing Treatments for Tuning the Wetting Properties of Carbon Nanotube Arrays.* Journal of Visualized Experiments : JoVE, 2013(74): p. 50378.

99. Kanbur, Y. and Z. Küçükyavuz, *Surface Modification and Characterization of Multi-Walled Carbon Nanotube.* Fullerenes, Nanotubes and Carbon Nanostructures, 2011. **19**(6): p. 497-504.

100. Maiti, S., et al., *A strategy for achieving low percolation and high electrical conductivity in melt-blended polycarbonate (PC)/multiwall carbon nanotube (MWCNT) nanocomposites: Electrical and thermo-mechanical properties.* Express Polymer Letters, 2013. **7**(6): p. 505-518.

101. Grossiord, N., et al., *High-Conductivity Polymer Nanocomposites Obtained by Tailoring the Characteristics of Carbon Nanotube Fillers.* Advanced Functional Materials, 2008. **18(**20): p. 3226-3234.

102. F.Y. Castillo, R.S., B. Krause, R. Headrick, B.P. Grady, R. Prada-Silvy and P. Pötschke, 2011. **52**.

103. Spears, C.P., *Volume doubling measurement of spherical and ellipsoidal tumors.* Medical and Pediatric Oncology, 1984. **12**(3): p. 212-217.

104. Lively, B., et al., *Quantified stereological macrodispersion analysis of polymer nanocomposites.* Composites Part A: Applied Science and Manufacturing, 2012. **43**(6): p. 847-855.

105. Sahagian, D.L. and A.A. Proussevitch, *3D particle size distributions from 2D observations: stereology for natural applications.* Journal of Volcanology and Geothermal Research, 1998. **84**(3–4): p. 173-196.